The quasar Main Sequence: recent developments

Paola Marziani[1]

E. Bon,[2] **N. Bon,**[2] **M. D'Onofrio**[3] **, M. Śniegowka**[4,5]**, B. Czerny**[4,5]**, S. Panda**[4,5]**,**

M. L. Martínez-Aldama[4]**, A. del Olmo**[6]**, C. A. Negrete**[7]**, D. Dultzin**[7]**, T. Buendia**[7] **,K. Garnica**[7]

[1]*INAF - Osservatorio Astronomico di Padova, Padova, Italia*

[2]*Astronomical Observatory, Belgrade, Serbia*

[3]*Dipartimento di Fisica ed Astronomia "Galileo Galilei", U. di Padova, Padova, Italia*

[4]*Nicolaus Copernicus Astronomical Center, Polish Academy of Sciences, Warsaw, Poland*

[5]*Center for Theoretical Physics, Polish Academic of Sciences, Warsaw, Poland*

[6]*Instituto de Astrofísica de Andalucía (CSIC), Granada, España*

[7]*Instituto de Astronomía, UNAM, México, D.F., México*

[6]*INAF - Osservatorio Astrofísica e Science dello Spazio, Bologna, Italia*

August 2021

SCSLSA 13

Introduction: a main sequence (MS) for type-1 (unobscured) quasars and its interpretation based on Eddington ratio and orientation

Population B extreme: fully disk- dominated quasars

Population A extreme: highly accreting quasars

The E1 main sequence (MS) is represented as an anti-correlation between strength of FeIIλ4570 and FWHM of Hβ (or peak intensity of [OIII] 4959,5007)

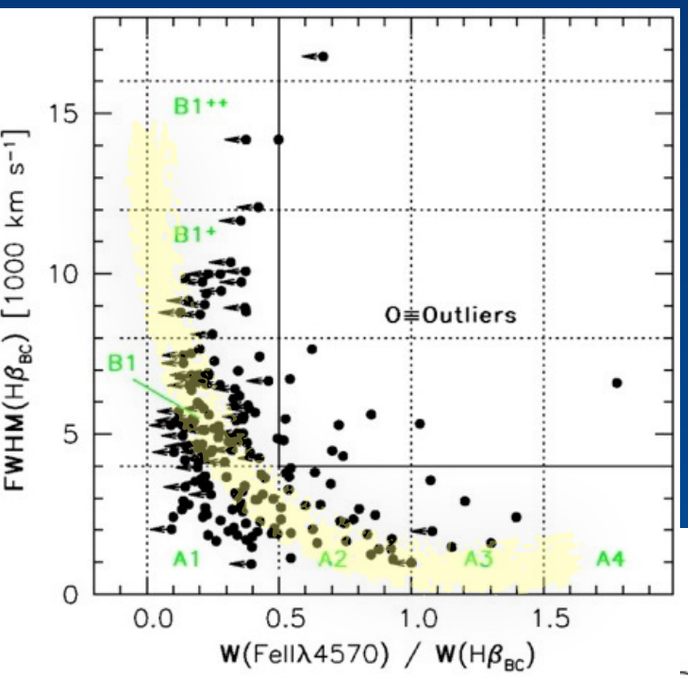

Sulentic et al. 2000, 2002;
n ~ 200

Eigenvector 1 (E1): originally defined by a Principal Component Analysis on the spectra of ~80 PG quasars

Boroson & Green 1992

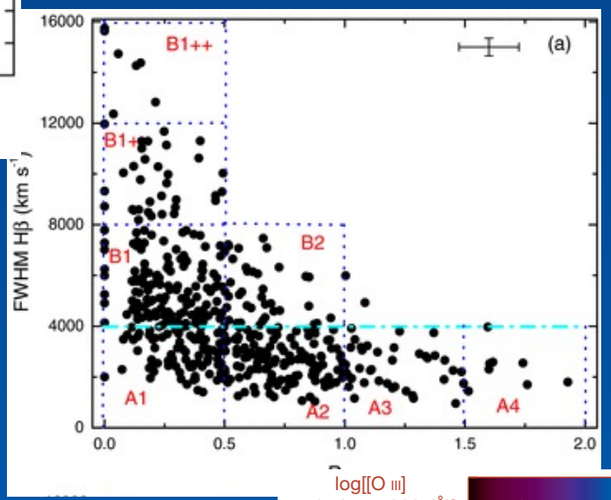

Zamfir et al. 2010, n ~ 500

Since 1992, the E1 MS has been found in increasingly larger samples

Shen & Ho 2014, n ~ 20000

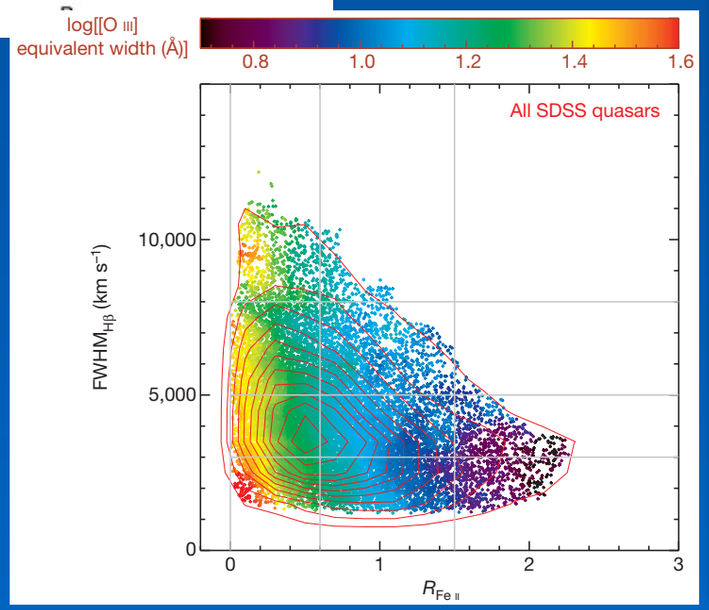

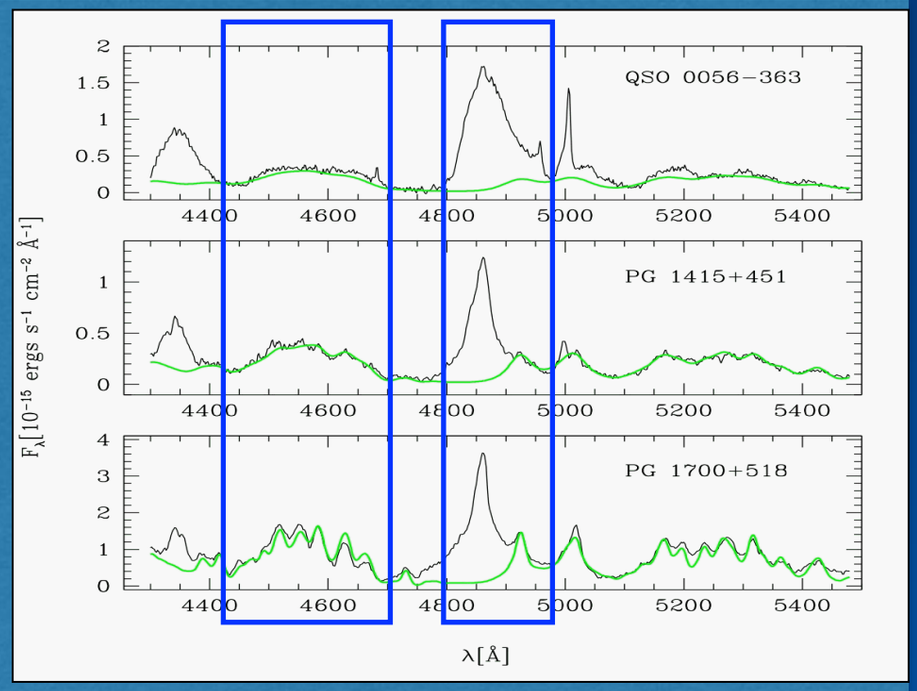

$$R_{\rm FeII} = \frac{I({\rm FeII}\lambda 4570)}{I(H\beta)} \approx \frac{W({\rm FeII}\lambda 4570)}{W(H\beta)}$$

FeII emission from UV to the IR can dominate the thermal balance of the low-ionization BLR

Marinello et al. 2018

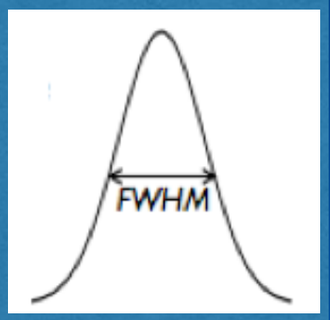

FWHM(Hβ): related to the velocity field in the low- ionization BLR (predominantly virialized)

Peterson & Wandel 2000;
recent reverberation studies

The elbow-shaped MS allows for the definition of two main populations (along with spectral types): Population A and B

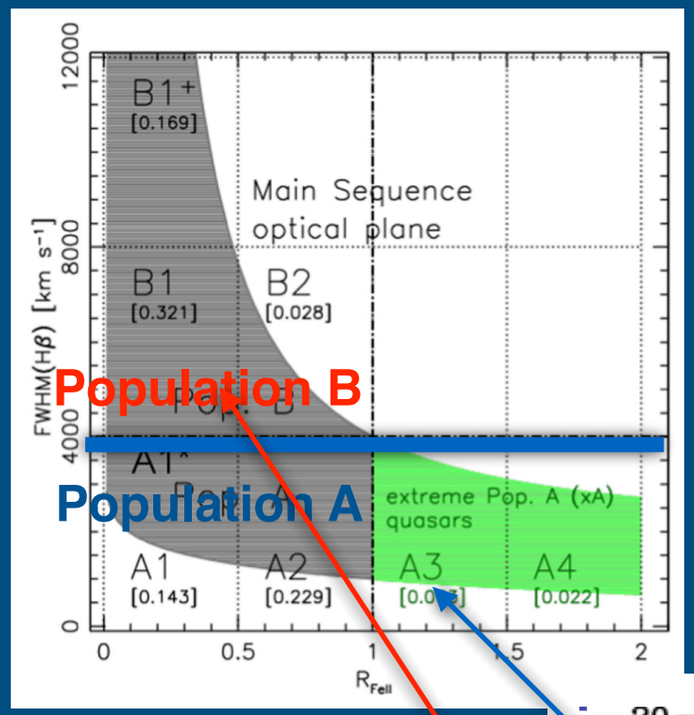

Population A (FWHM(Hβ) ≲ 4000 km s^{-1}):
low ionization lines symmetric and unshifted → virial equilibrium
large CIV blueshifts → prominent outflows

Population B (FWHM(Hβ) ≳ 4000 km s^{-1}):
low ionization emission often red-ward symmetric;
reverberation mapping → stratification and virial equilibrium

Sulentic et al. 2000; Population 1 and 2: Collin et al. 2006;
Disk and wind dominated: Richards et al. 2002

Key multifrequency parameters related to the accretion process and the accompanying outflows show a trend along the MS

Summary Table in Fraix-Burnet et al. 2017; see also Marziani et al. 2018

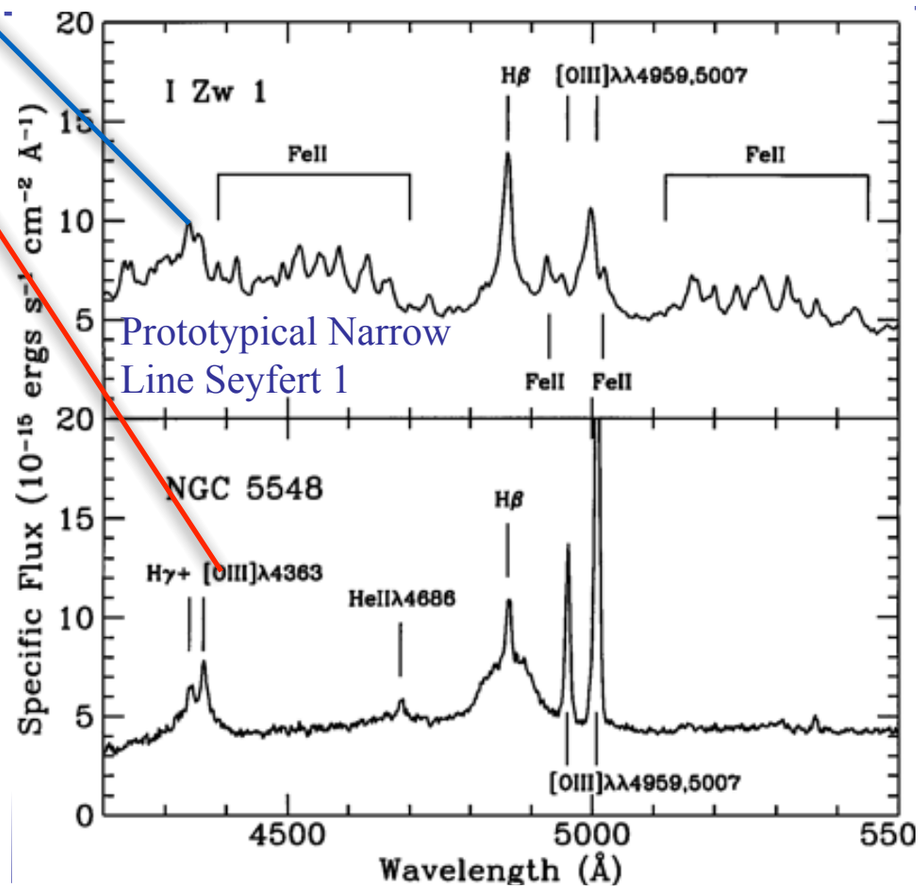

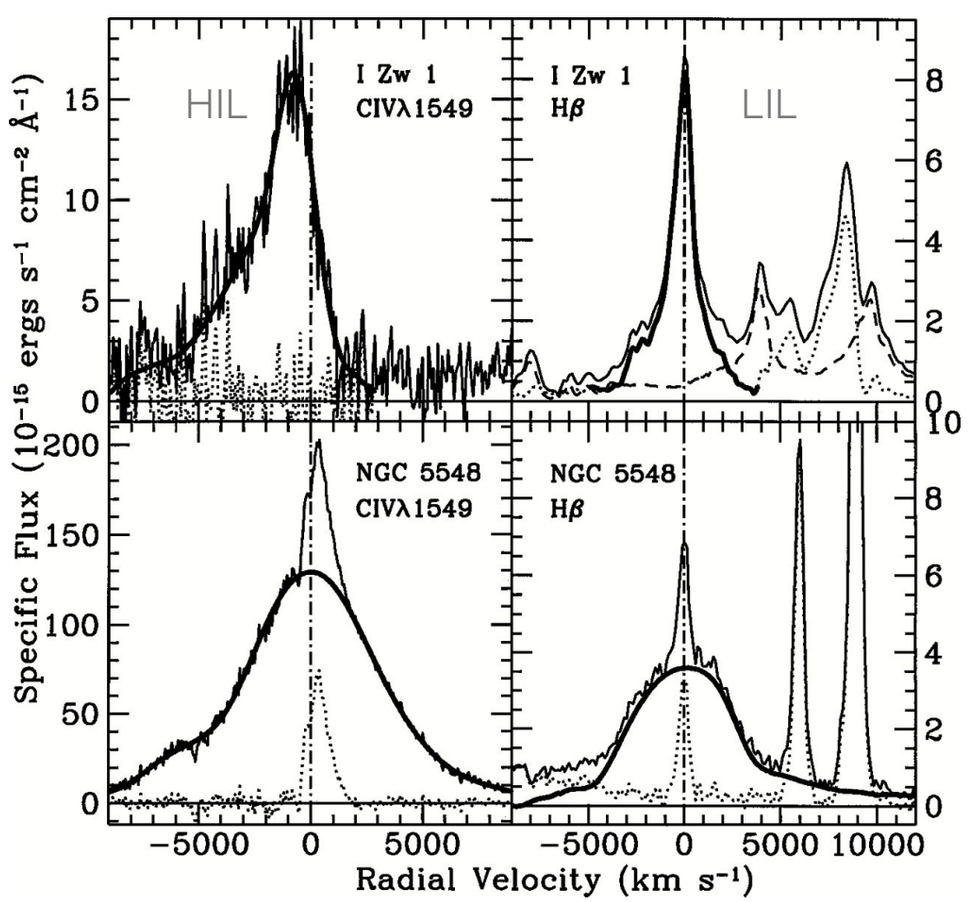

Hβ profiles remain Lorentzian-like up to around FWHM(Hβ) = 4000 km s^{-1}

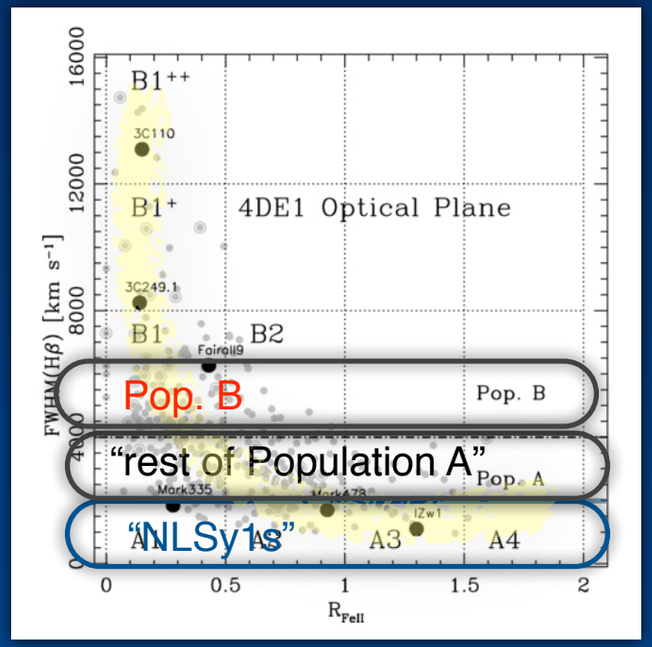

NLy1s (FWHM(Hβ) < 2000 km s^{-1})
vs "rest of Population A":
2000 km s^{-1} < FWHM(Hβ) < 4000 km s^{-1}

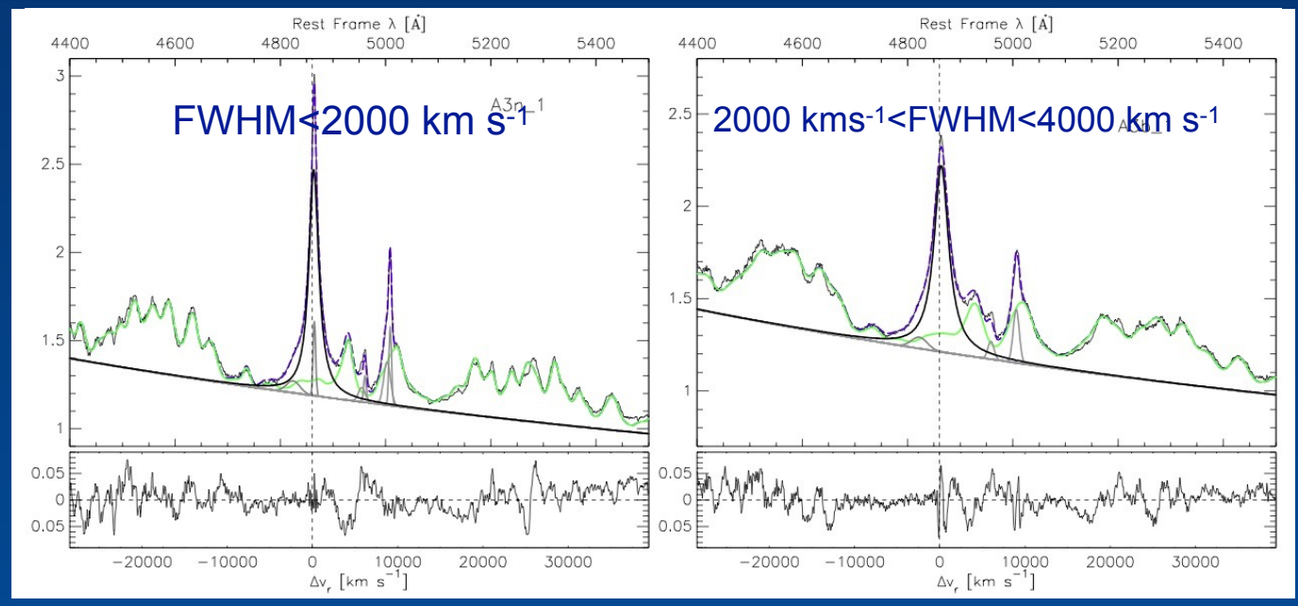

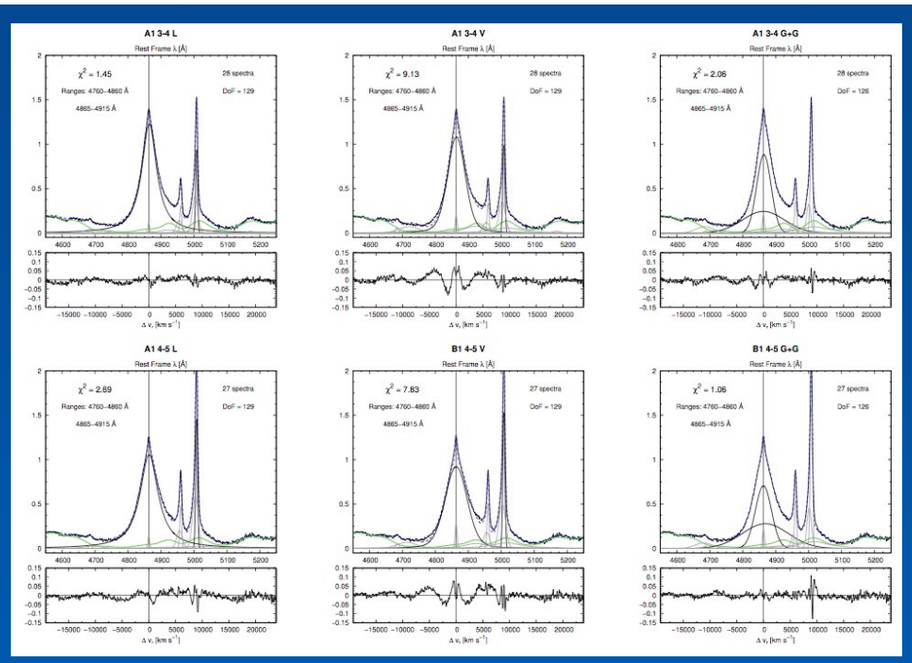

χ^2~1.45

Lorentzian Population A

χ^2~2.69

3000<FWHM<4000

χ^2~2.06

4000<FWHM<5000

χ^2~1.06

Double Gaussian Population B

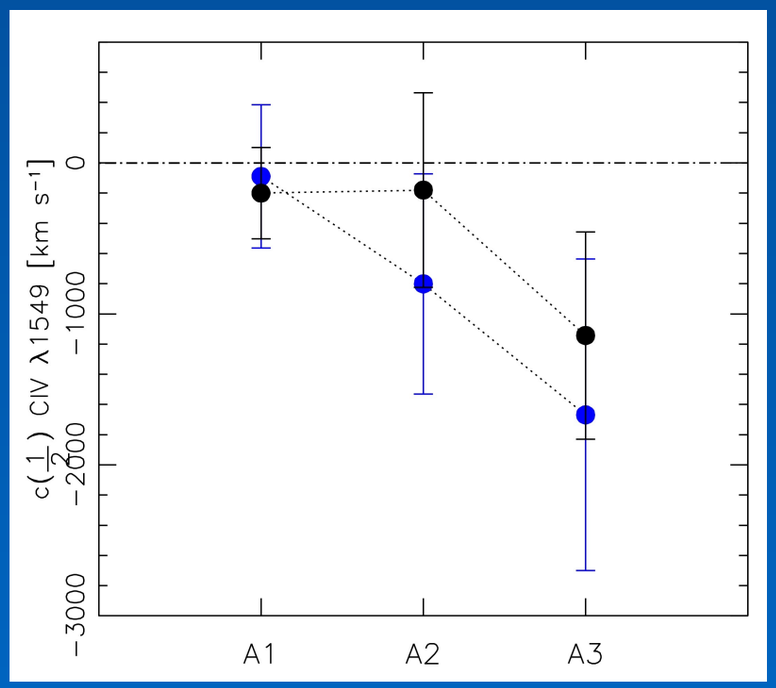

CIV blueshifts among NLSy1s increase with R_{FeII} but remain consistent up to FWHM(Hβ) = 4000 km s^{-1}

Negrete et al. 2018; Marziani et al. 2018, and in preparation; cf. Cracco et al. 2016

Several approaches consistently support a relation between L/L_{Edd} and R_{FeII}

The M_{BH} proxy $\sigma_\star$ decreases with R_{FeII} in narrow luminosity bins $\Rightarrow L/L_{Edd}$ increases with R_{FeII}

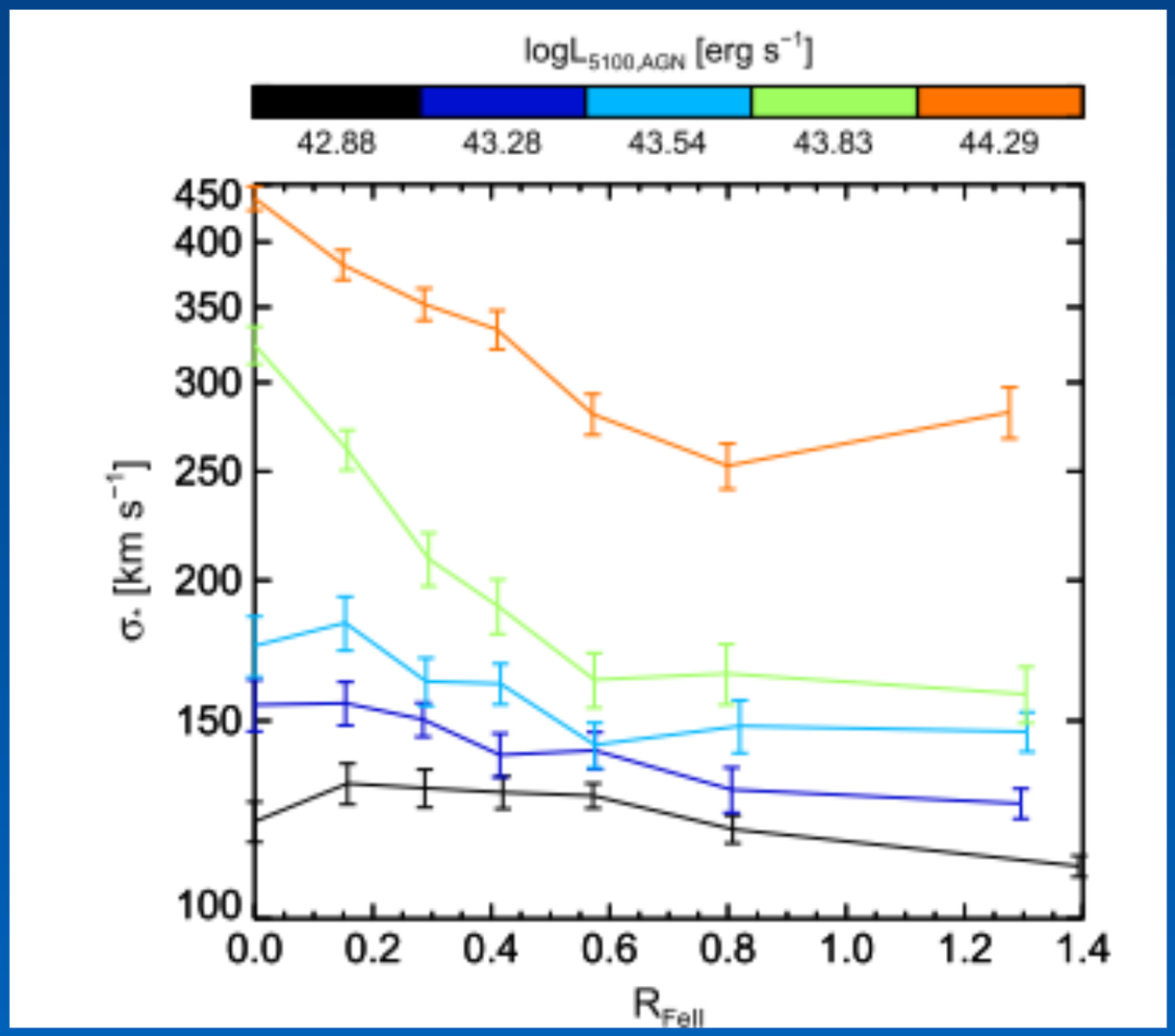

Sun & Shen 2015

Fundamental plane of accreting massive black holes

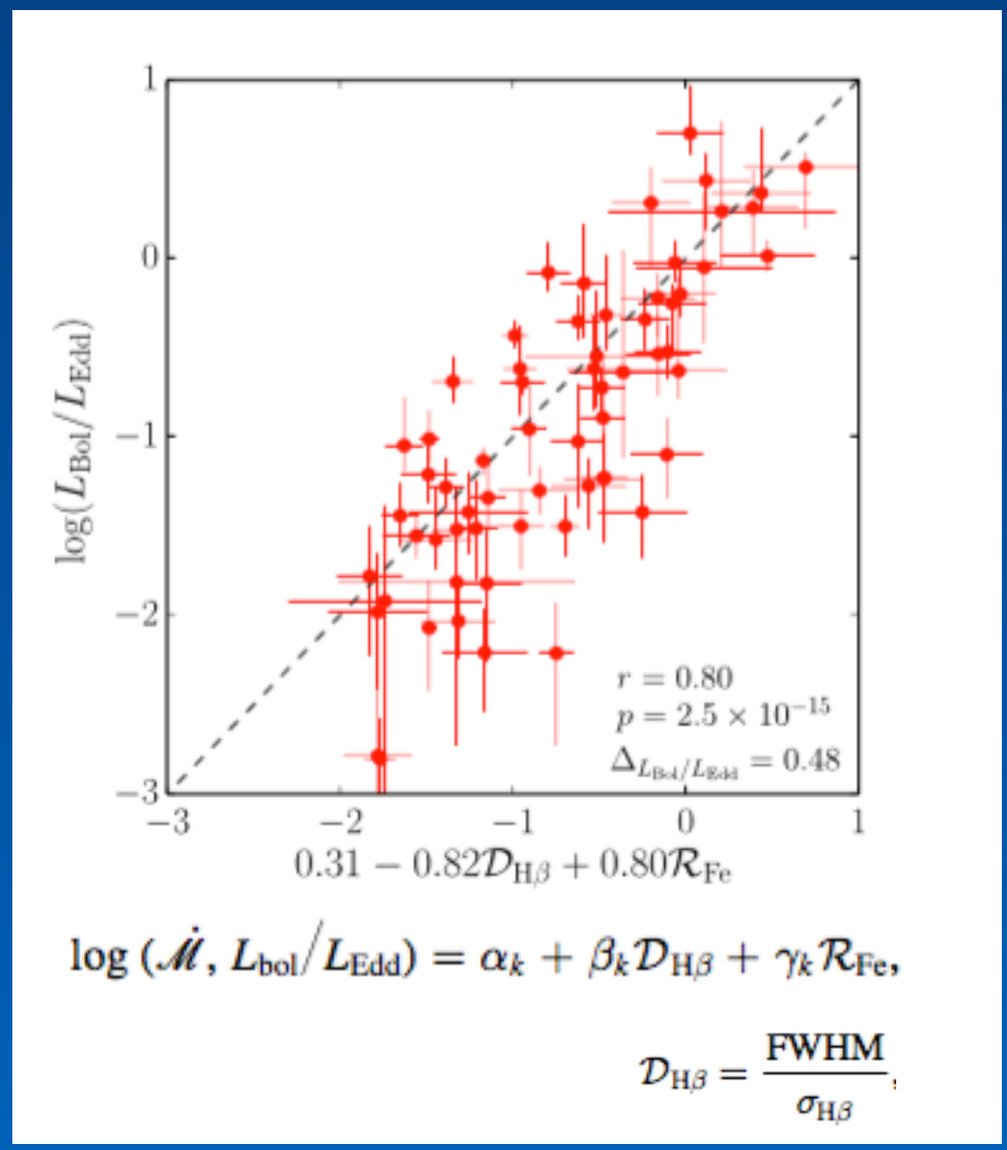

Du et al. 2016, assumed virial relation

Occupation of the MS optical plane at low-z can be accounted for in terms of Eddington ratio and orientation

- Population A: $L/L_{Edd} \gtrsim 0.1$-0.2
- Population B $L/L_{Edd} \lesssim 0.1$-0.2
- Pop. A includes rare ($P(\theta) \propto \sin\theta$) lower L/L_{Edd} face-on sources
- NLSy1s preferentially sample face-on sources along the MS

Key assumptions: $R_{FeII} \propto L/L_{Edd}$ Virial velocity field in a flattened geometry

$$M_{BH} = f(\theta) r_{BLR} FWHM^2/G$$

$$FWHM \propto M_{BH}^{1/4} (L/L_{Edd})^{-1/4} f(\theta)^{-1/2} \text{ (virial)};$$

$$R_{FeII} \propto R_{FeII}(L/L_{Edd}) \cos\theta (1 + b \cos\theta)$$

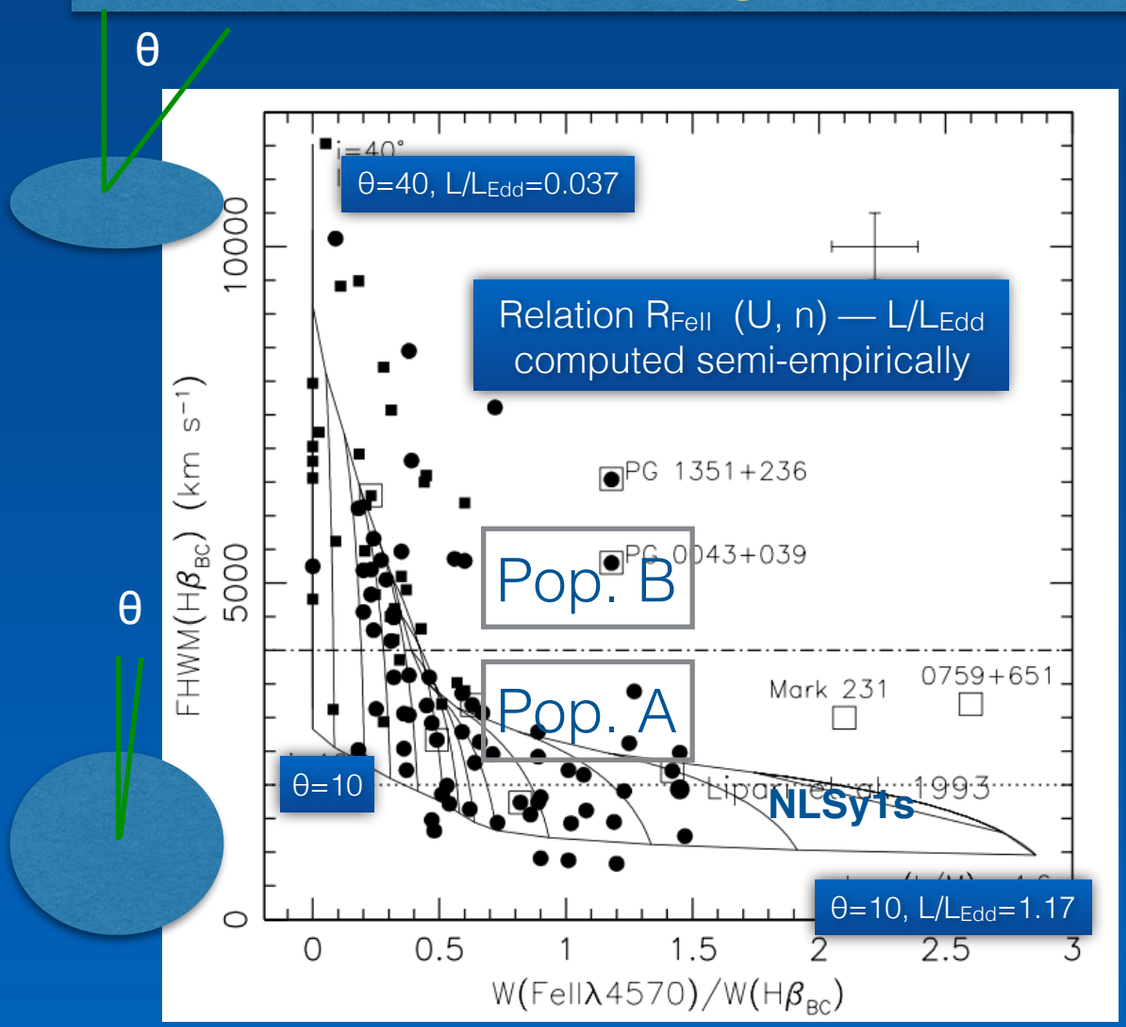

Marziani et al. 2001; Marziani et al. 2018

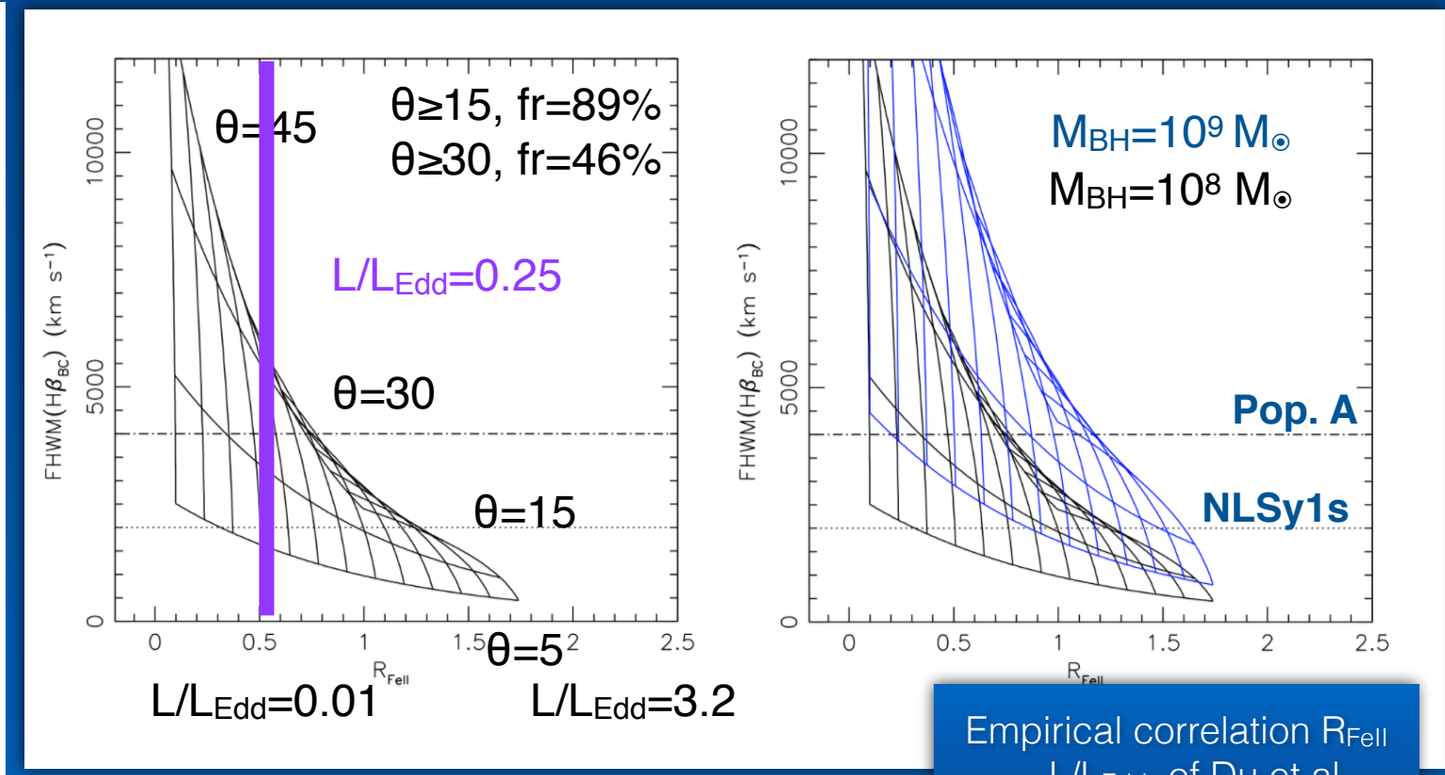

Empirical correlation R_{FeII} — L/L_{Edd} of Du et al. (2016)

Increasing Black hole mass displaces the sequence upward

The relative occupation in the $R_{Fe\,II}$ sequence *is* explained as a sequence of increasing L/L_{Edd} and related observational trends i.e., cloud density n_H, chemical composition Z, and SED shape.

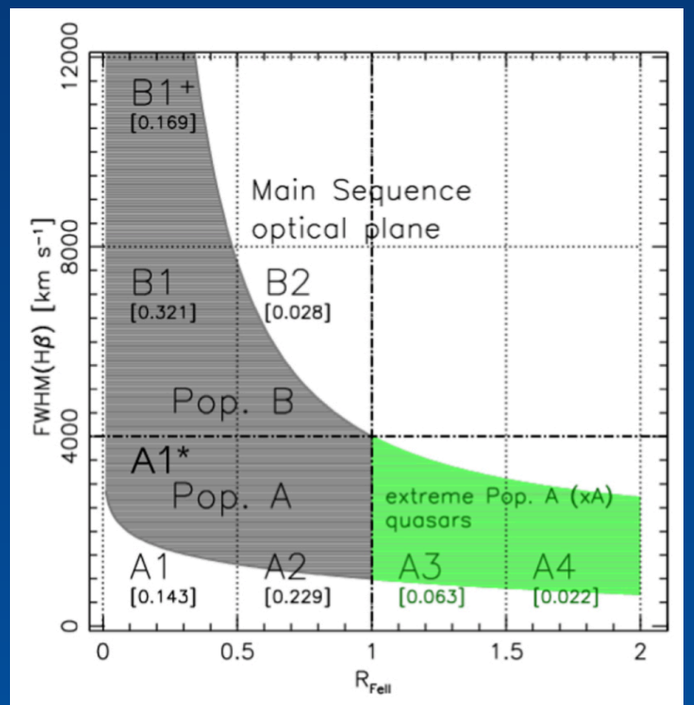

B and A1: relatively low density, low Z, and low L/L_{Edd}

A2: moderate density $n_H \sim 10^{11}$ cm^{-3}, intermediate L/L_{Edd} , $Z \sim 5Z_\odot$

$R_{FeII} > 1$: higher n_H, radiative output at the $L/L_{Edd} \sim 1$, and $Z \gtrsim 10Z_\odot$

B1++ cannot be accounted for $M_{BH}=10^8\ M_\odot$

R_{FeII} predicted from Cloudy 17.02 model as a function of R_{BLR}

Panda et al. 2019

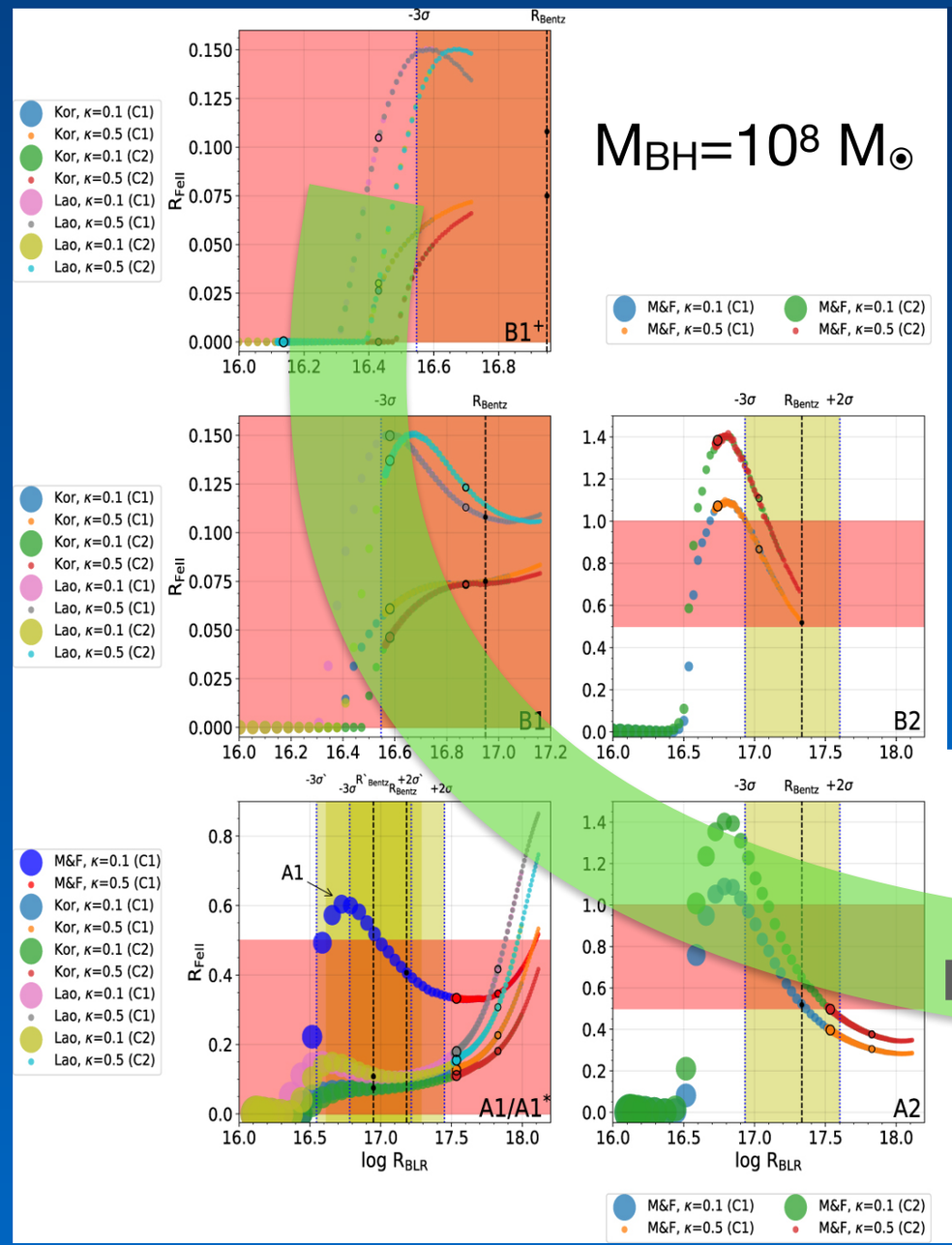

$M_{BH}=10^8\ M_\odot$

$M_{BH} = f(\theta) r_{BLR}\ FWHM^2/G$

$f(\theta) = 1/[4(\kappa^2+\sin^2\theta)]$

$\delta v_K^2 = f(\theta) FWHM^2$

$\kappa = \delta v_{iso}/\delta v_K$

each bin assumes fixed L/L_{Edd}, n_H, Z, SED

n_H, Z, L/L_{Edd}

Extreme Population B

very broad Balmer profiles, low R_{FeII}, low accretion rate

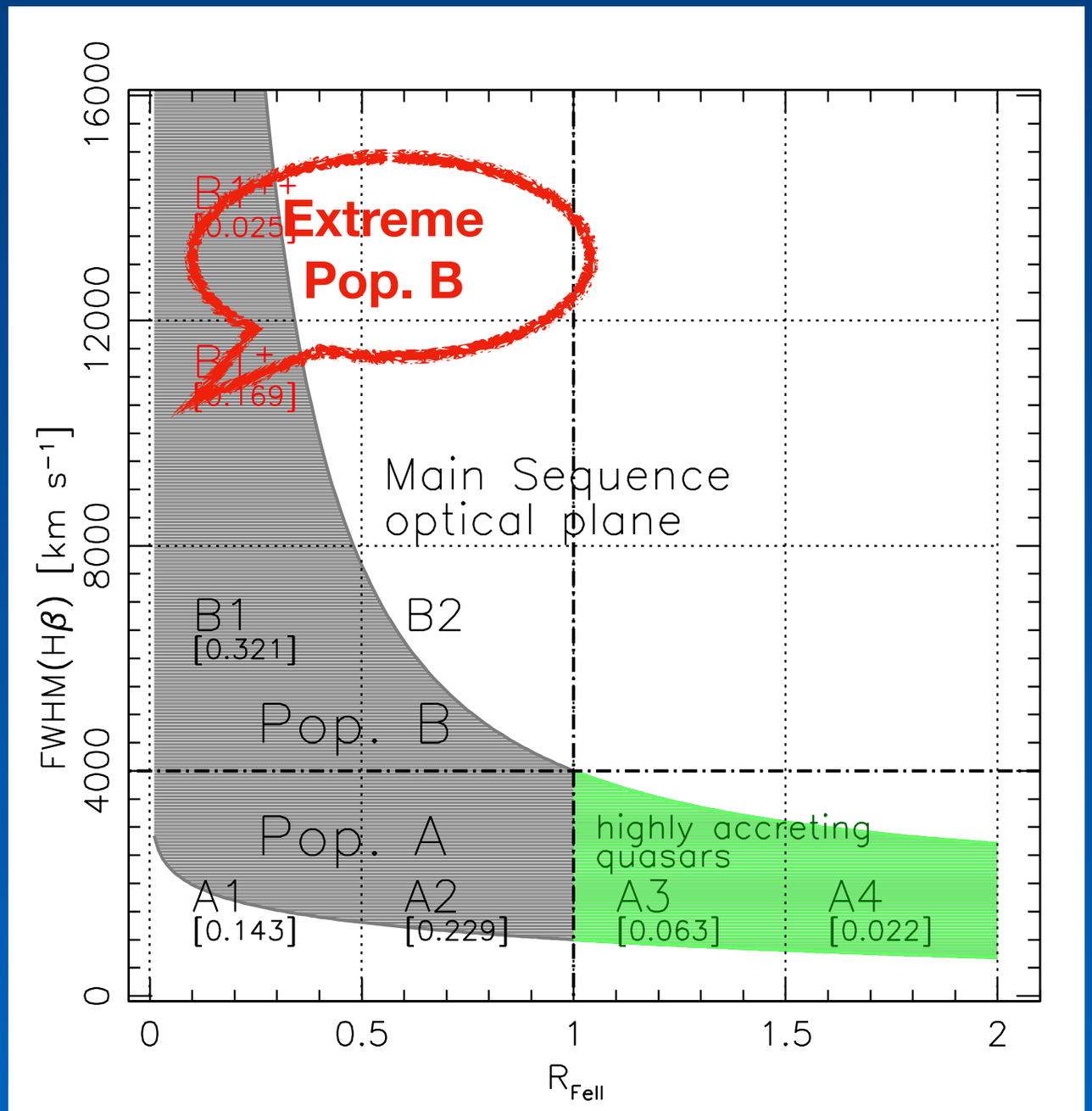

NGC 1275: broad line region chemical composition analysis

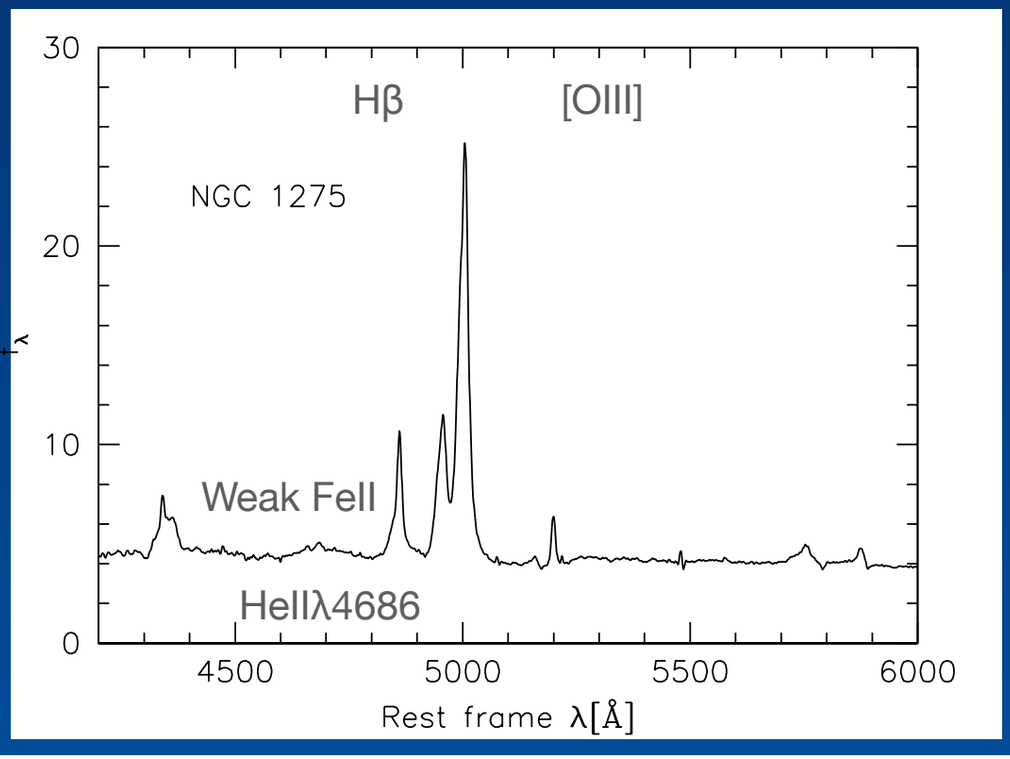

Detection and isolation of relatively faint broad components

Constraints: Very weak FeII, prominent HeIIλ4686, low CIVλ1549/HeIIλ1640 ratio

Broad components of HeIIλ4686, Hβ (Copernico), CIVλ1549, HeIIλ1640 (HST COS)

Punsly et al. 2018

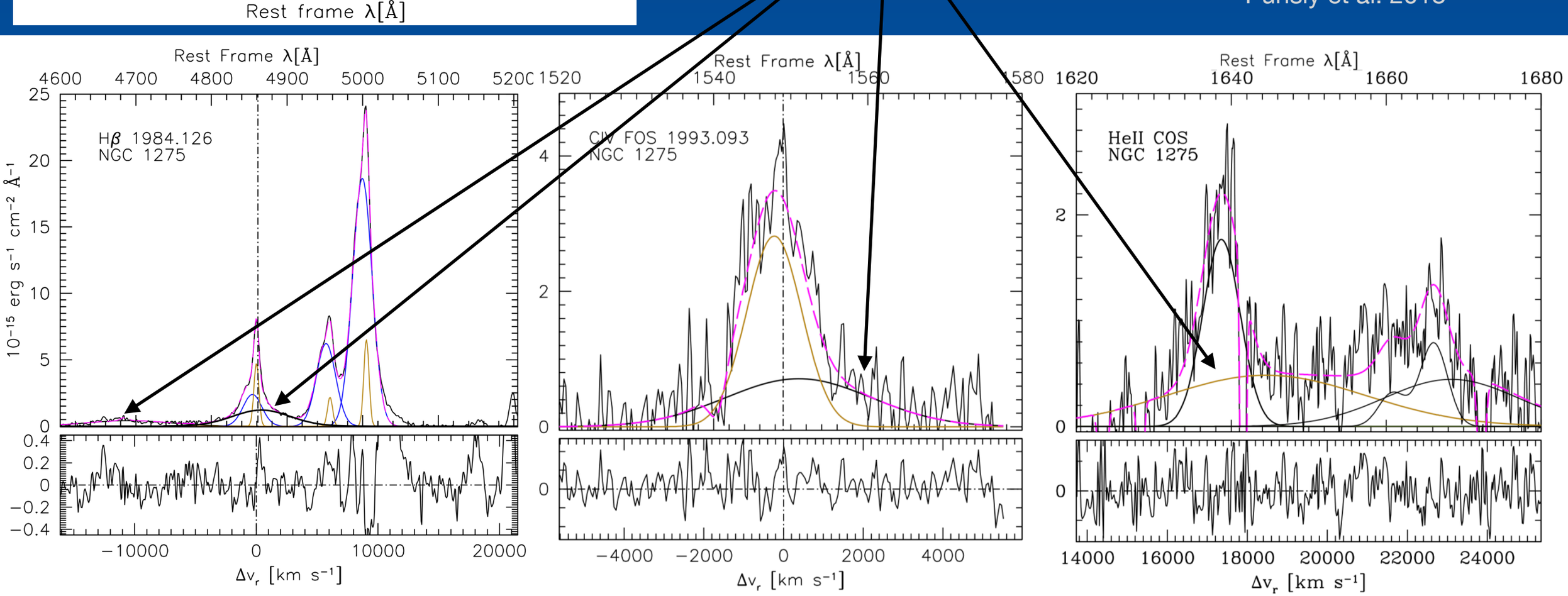

NGC 1275: solar or slightly subsolar metallicity, $0.1\ Z_\odot \lesssim Z \lesssim 1\ Z_\odot$

$$\frac{L(\text{C IV})}{L(\text{H}\beta)} = 0.3 - 0.8,\ \frac{L(\text{P}\alpha)}{L(\text{H}\beta)} = 0.6 - 1.1,$$
$$\frac{L(\text{Fe II})}{L(\text{H}\beta)} < 0.3,$$
$$\frac{L(\text{He II}\lambda 1640)}{L(\text{C IV})} = 0.5 - 1.0.$$

Moderate density $n_H \sim 10^{10}$ cm^{-3}, and column density $N_H \sim 10^{23}$ cm^{-2}.

Exploration of a parameter subspace in n_H, ionization parameter U, N_H, metallicity, with CLOUDY 17.01 assuming a carefully defined SED

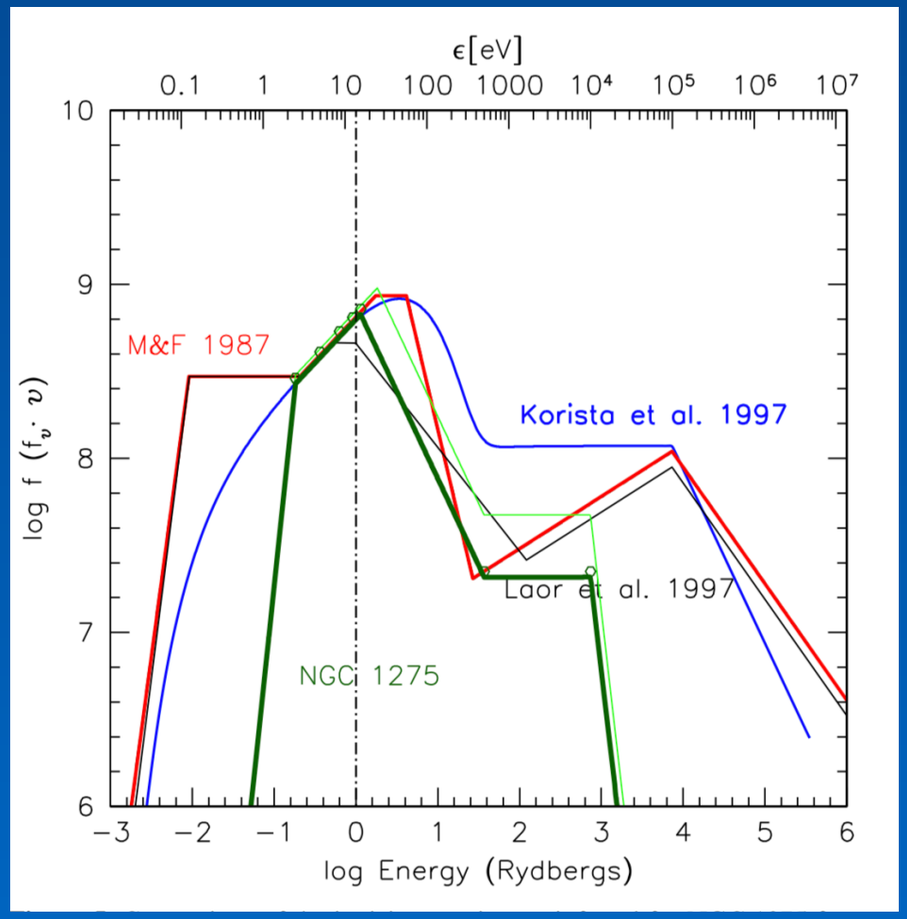

Table 2
CLOUDY Simulations: NGC 1275

1	2	3	4	5	6	7	8	9	10	11
Z	$\log n$	$\log N_H$	$\log r$	$\log U$	$\log L(\text{H}\beta)$	C IV/Hβ	Pα/Hβ	He II/C IV	Fe II/Hβ	Conformance
Metalicity	Number Density cm^{-3}	Column Density cm^{-2}	Radius cm	Ionization Parameter	Luminosity erg s^{-1}	Target 0.3–0.8	Target 0.6–1.1	Target 0.5–1.0	Target <0.3	
0.1	9.75	22.7	16.5	−1.24	40.76	1.63	0.99	0.44	0.03	No
0.1	9.75	23.3	16.5	−1.24	40.80	1.47	1.09	0.43	0.06	No
0.1	9.75	22.7	16.75	−1.74	40.76	1.63	0.99	0.44	0.03	No
0.1	9.75	23.3	16.75	−1.74	40.80	1.47	1.09	0.43	0.06	No
0.1	9.75	22.7	17.0	−2.24	40.76	1.63	0.99	0.44	0.03	No
0.1	9.75	23.3	17.0	−2.24	40.80	1.47	1.09	0.43	0.06	No
0.1	10.0	22.7	16.5	−1.49	40.81	0.63	0.92	0.99	0.02	Yes
0.1	10.0	23.3	16.5	−1.49	40.84	0.59	1.01	0.97	0.05	Yes
0.1	10.0	22.7	16.75	−1.99	40.81	0.63	0.91	0.99	0.02	Yes
0.1	10.0	23.3	16.75	−1.99	40.84	0.59	1.01	0.97	0.05	Yes
0.1	10.0	22.7	17.0	−2.49	40.81	0.63	0.91	0.99	0.02	Yes
0.1	10.0	23.3	17.0	−2.49	40.84	0.59	1.01	0.97	0.05	Yes
0.1	10.25	22.7	16.5	−1.74	40.87	0.20	0.84	2.64	0.02	No
0.1	10.25	23.3	16.5	−1.74	40.89	0.19	0.93	2.59	0.04	No
0.1	10.25	22.7	16.75	−2.24	40.87	0.20	0.84	2.64	0.02	No
0.1	10.25	23.3	16.75	−2.24	40.89	0.19	0.93	2.59	0.04	No
0.1	10.25	22.7	17.0	−2.74	40.87	0.20	0.84	2.64	0.02	No
0.1	10.25	23.3	17.0	−2.74	40.89	0.19	0.93	2.59	0.04	No
0.1	10.5	22.7	16.5	−1.99	40.93	0.06	0.77	8.22	0.02	No
0.1	10.5	23.3	16.5	−1.99	40.94	0.05	0.87	8.08	0.03	No
0.1	10.5	22.7	16.75	−2.49	40.93	0.06	0.77	8.22	0.02	No
0.1	10.5	23.3	16.75	−2.49	40.94	0.05	0.87	8.08	0.03	No
0.1	10.5	22.7	17.0	−2.99	40.93	0.06	0.77	8.22	0.02	No
0.1	10.5	23.3	17.0	−2.99	40.94	0.05	0.87	8.08	0.03	No
1.0	9.75	22.7	16.5	−1.24	40.75	11.8	0.33	0.07	0.04	No
1.0	9.75	23.3	16.5	−1.24	40.83	9.77	0.35	0.07	0.07	No
1.0	9.75	22.7	16.75	−1.74	40.82	7.67	0.60	0.08	0.08	No
1.0	9.75	23.3	16.75	−1.74	40.89	6.49	0.54	0.08	0.11	No
1.0	9.75	22.7	17.0	−2.24	40.76	3.85	1.02	0.18	0.19	No
1.0	9.75	23.3	17.0	−2.24	40.78	3.65	1.05	0.18	0.27	No
1.0	10.0	22.7	16.5	−1.49	40.71	11.2	0.32	0.07	0.05	No
1.0	10.0	23.3	16.5	−1.49	40.77	9.72	0.36	0.07	0.08	No
1.0	10.0	22.7	16.75	−1.99	40.85	5.20	0.52	0.11	0.07	No
1.0	10.0	23.3	16.75	−1.99	40.88	4.84	0.56	0.11	0.11	No
1.0	10.0	22.7	17.0	−2.49	40.79	1.91	0.97	0.32	0.22	No
1.0	10.0	23.3	17.0	−2.49	40.81	1.84	1.00	0.32	0.22	No
1.0	10.25	22.7	16.5	−1.74	40.69	9.33	0.35	0.09	0.06	No
1.0	10.25	23.3	16.5	−1.74	40.73	8.40	0.34	0.09	0.09	No
1.0	10.25	22.7	16.75	−2.24	40.81	3.55	0.55	0.17	0.08	No
1.0	10.25	22.7	17.0	−2.74	40.83	0.76	0.91	0.73	0.12	Yes
1.0	10.25	23.3	17.0	−2.74	40.85	0.73	0.94	0.73	0.18	Yes
1.0	10.5	23.3	16.5	−1.99	40.68	6.86	0.41	0.13	0.11	No
1.0	10.5	22.7	16.75	−2.49	40.82	1.85	0.54	0.32	0.08	No
1.0	10.5	23.3	16.75	−2.49	40.83	1.81	0.54	0.32	0.12	No
1.0	10.5	22.7	17.0	−2.99	40.88	0.23	0.84	2.09	0.10	No
1.0	10.5	23.3	17.0	−2.99	40.89	0.22	0.84	2.09	0.15	No

Extreme Population B: accretion disk emission lines

Candidate accretion disk profiles
Few (~ 2% in the SDSS),
very broad Population B sources
show a double peaked Balmer line profile

Eddington ratios are low
much lower than those of
typical type-1 AGN: < 0.02;
AD "bared": extreme Population B

Arp 102B: $M_R \sim -25.7$
$R_{FeII} \lesssim 0.1$
$L/L_{Edd}<0.1$

UNAM KIAS 613: $M_z > -21.9$
$R_{FeII} \lesssim 0.1$
$L/L_{Edd} \ll 0.1$

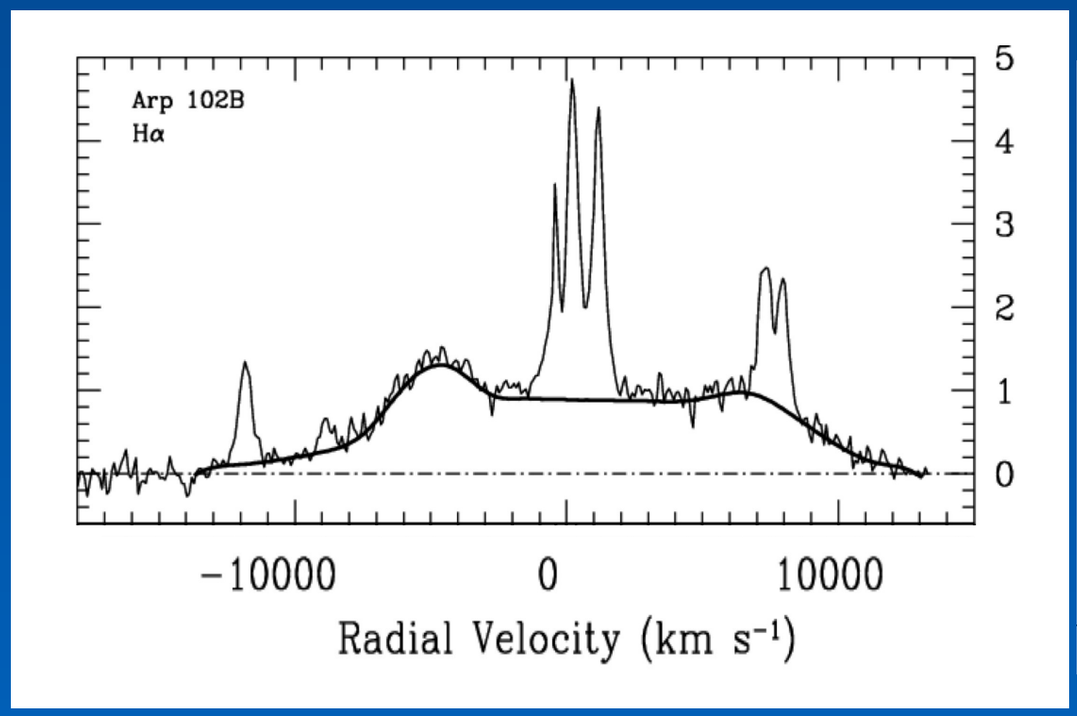

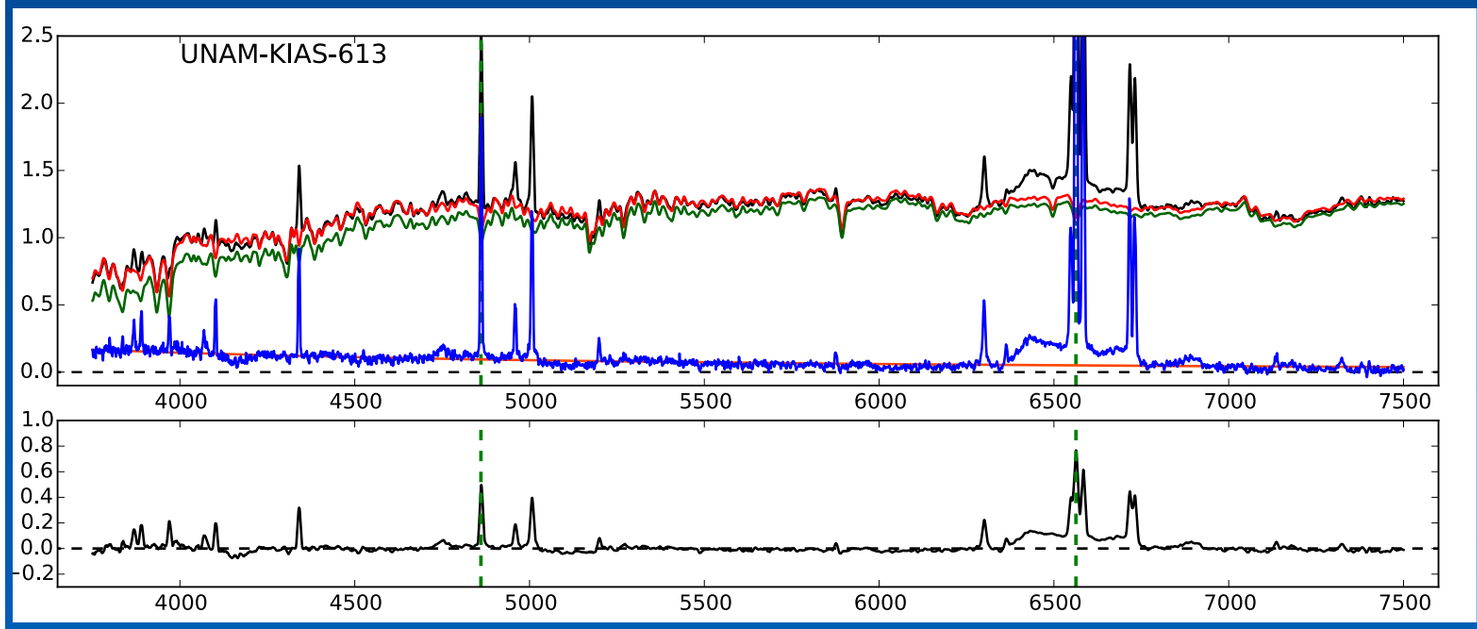

Sulentic et al. 2000; Strateva et al. 2003, 2007

Hernandez-Toledo et al. in preparation

Blazar line profiles consistent with contribution from accretion disk

AD parameters: $\theta \lesssim 5$, inner radius $\lesssim 100\ r_g$

AD emission favoured by the low level of the ionizing continuum

Extreme Pop. B red wing asymmetry
accounted for by gravitational and transverse redshift

$$\delta z_{\rm grav} = \frac{3}{2}\frac{r_{\rm g}}{r}$$

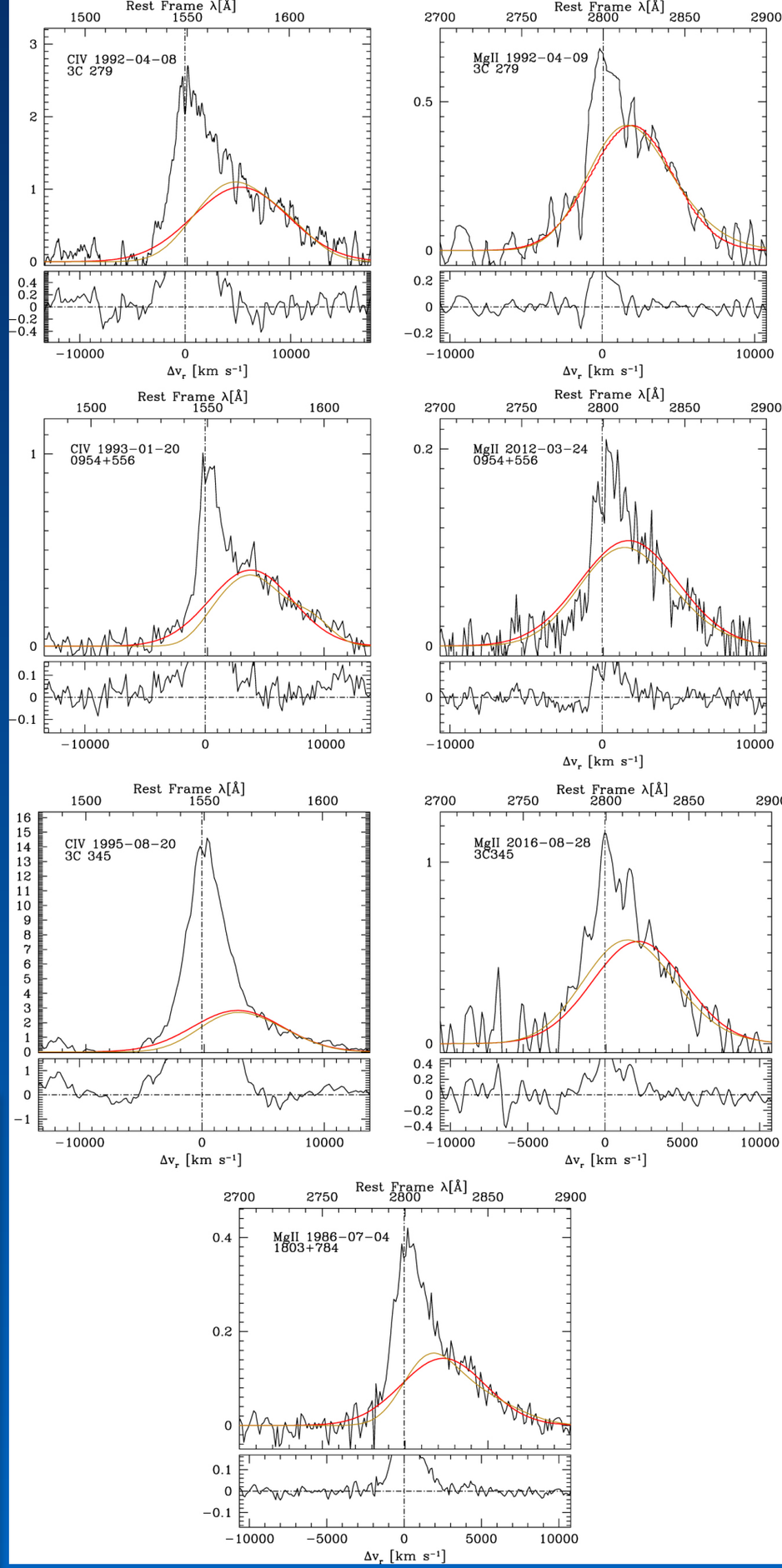

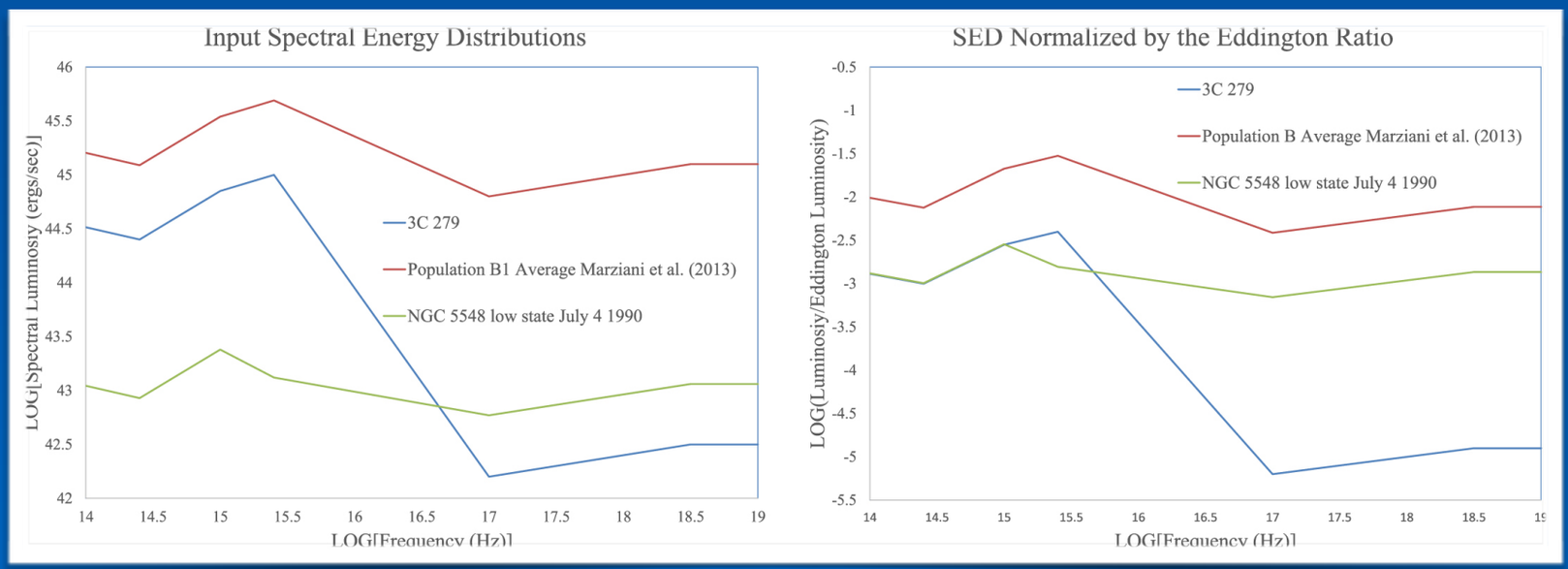

Orientation effects are at a play for low Eddington ratio

More in the talk by Edi Bon at this conference

Candidate accretion disk profiles also show shifts at the line base consistent gravitational and transverse redshift. Disk models suggest higher orientation.

Is the gravitational redshift hypothesis is applicable to most Population B sources?

Popovic et al. 1995; Corbin 1995; Bon et al. 2015

Contribution of a wind component and additional emission in the BC can complicate the issue

Popovic et al. 2004; Bon et al. 2009

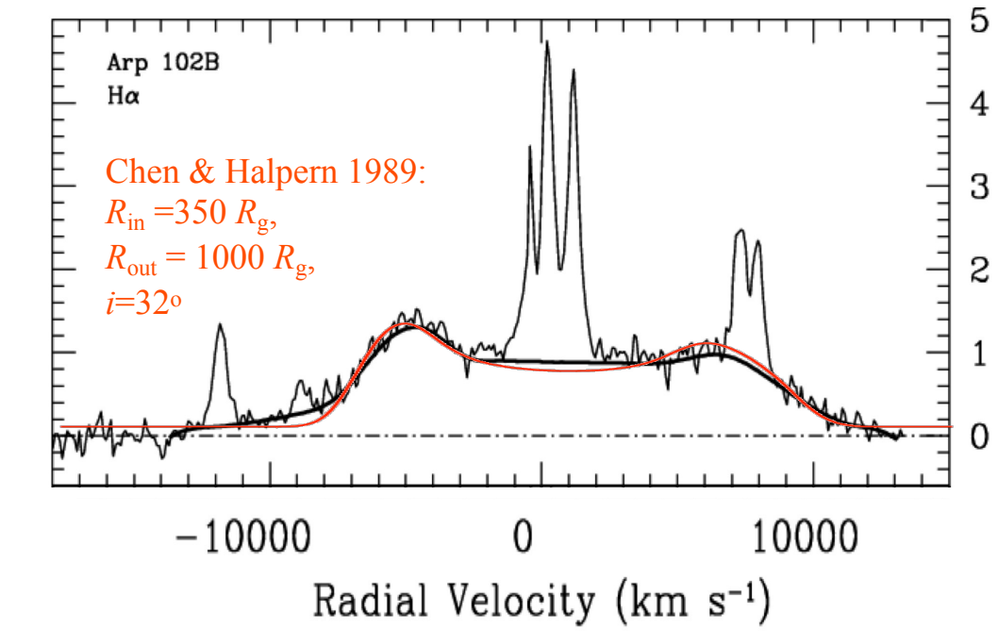

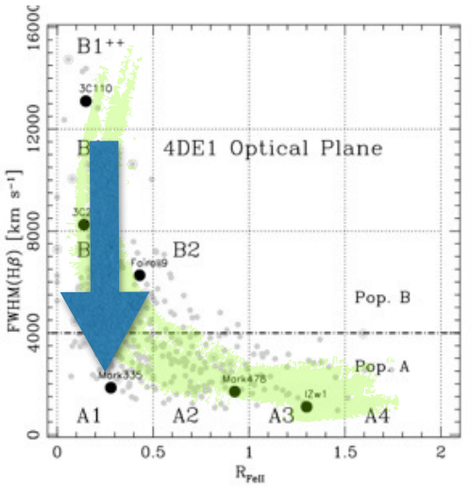

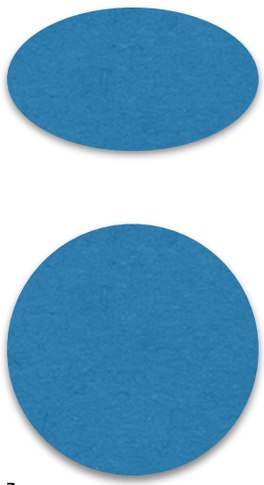

θ=30-50

θ≲5

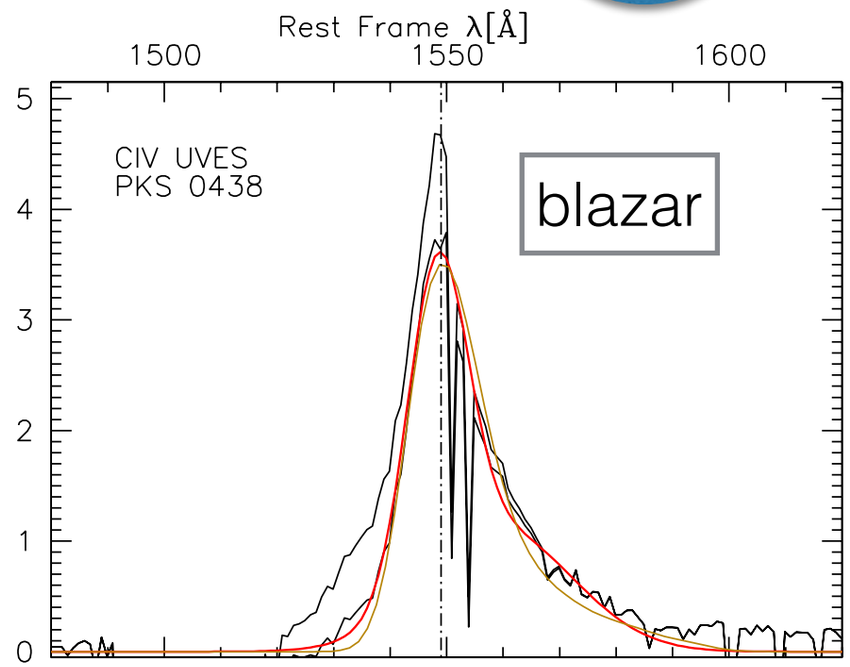

Extreme Population A

Highly accreting, possibly super-Eddington quasars

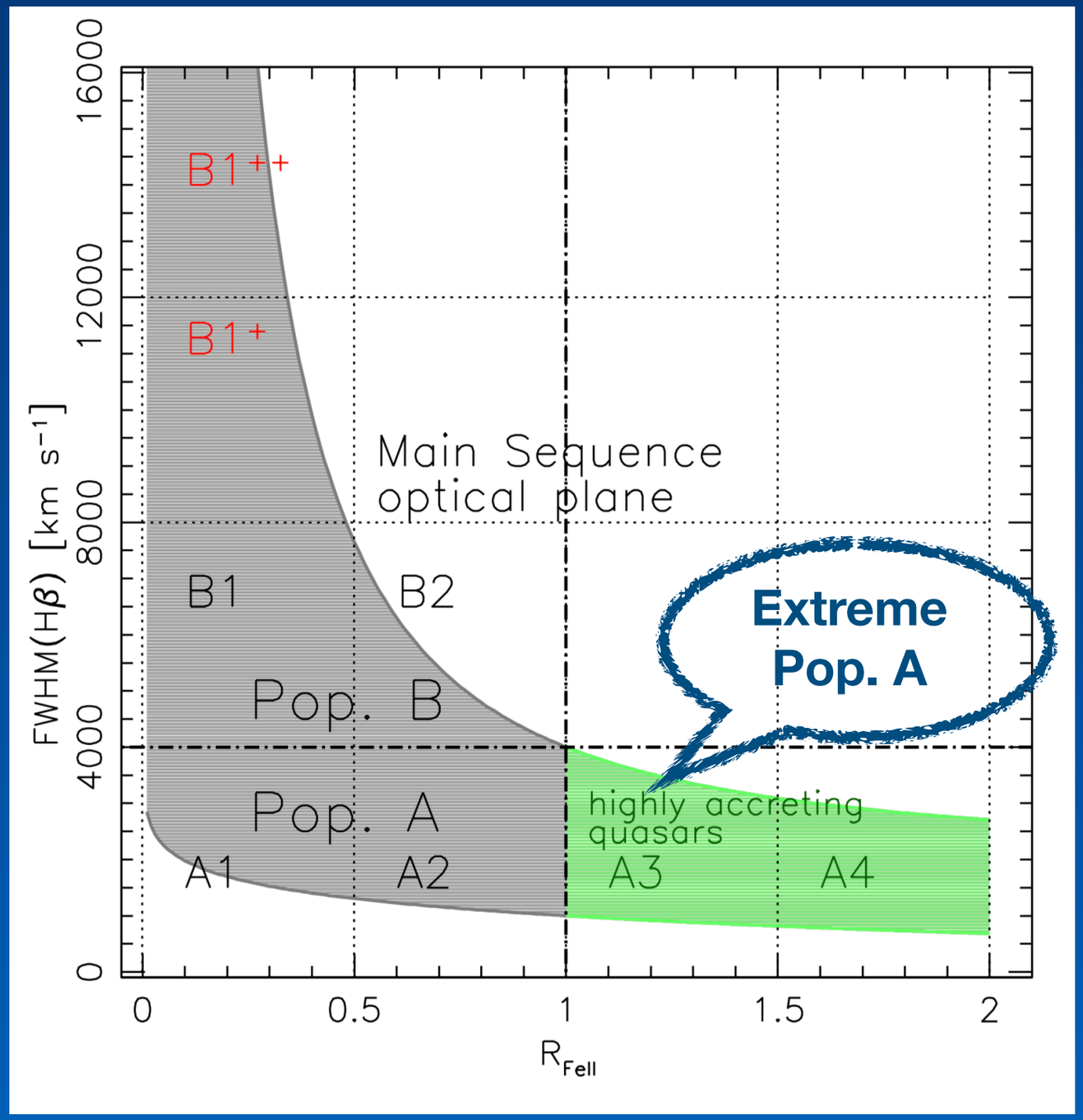

Extreme Population A: low ionisation emitting region + high ionization wind (truly "wind-dominated")

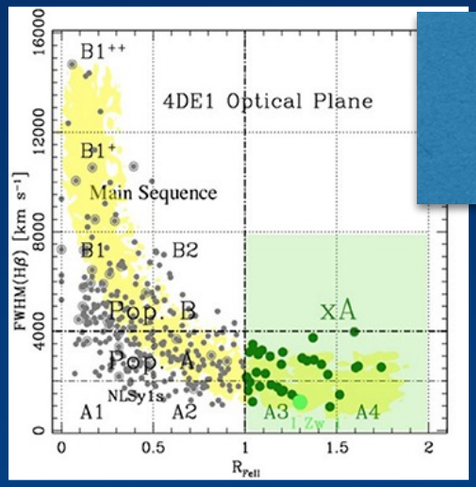

Extreme Pop. A (xA; R_{FeII}>1): CIVλ1549 mainly blueshifted (I.e.) wind emission but Balmer and Paschen lines remain predominantly virialized

UV selection criteria from diagnostic line ratios corresponding to R_{FeII} > 1.0:
UV AlIII λ1860/SiIII]λ1892>0.5 &
SiIII]λ1892/ CIII]λ1909>1
imply strong AlIII λ1860 and weak CIII]λ1909

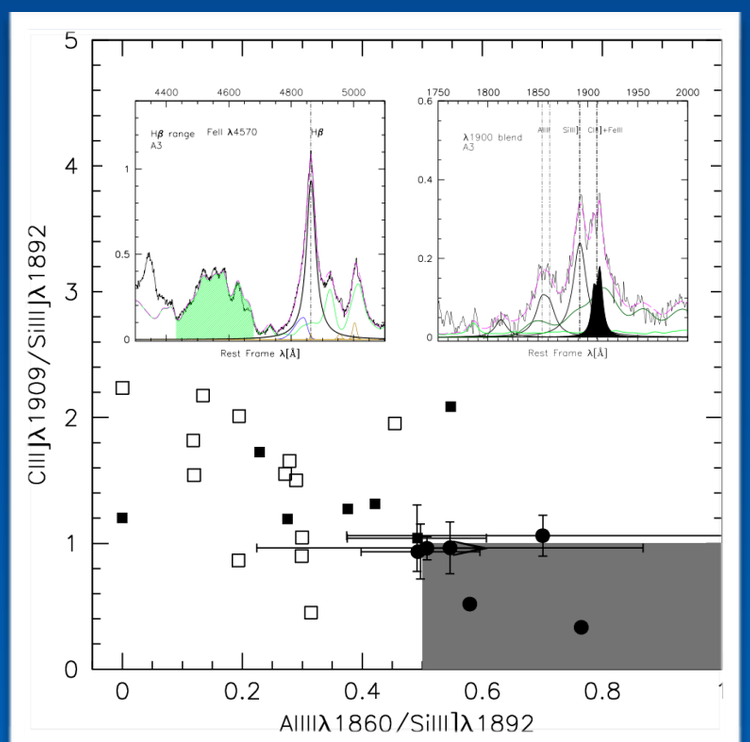

UV and optical selection criteria

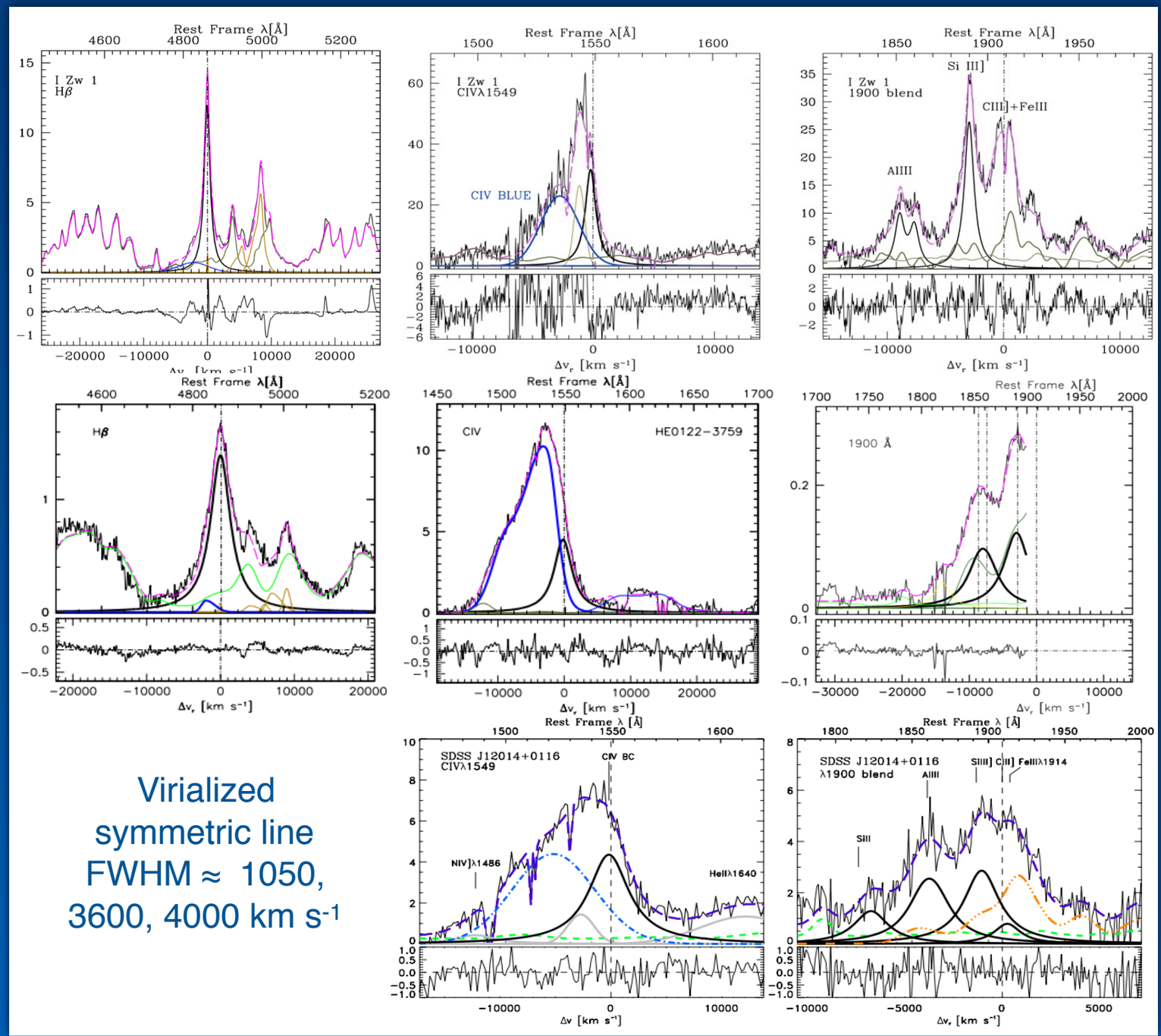

Virialized symmetric line FWHM ≈ 1050, 3600, 4000 km s^{-1}

Marziani & Sulentic 2014; Dultzin et al. 2020; more in Tania Buendia's talk

The diagnostics applied to xA spectra show a fairly monotonic trend with metallicity Z

Diagnostic line ratios
CIVλ1549/HeIIλ1640
AlIII λ1860/HeIIλ1640
(SiIV+OIV])λ1400/
HeIIλ1640

HeIIλ1640 expedient because of "constant" He abundance and of simple HeIIλ1640 radiation transfer but very weak

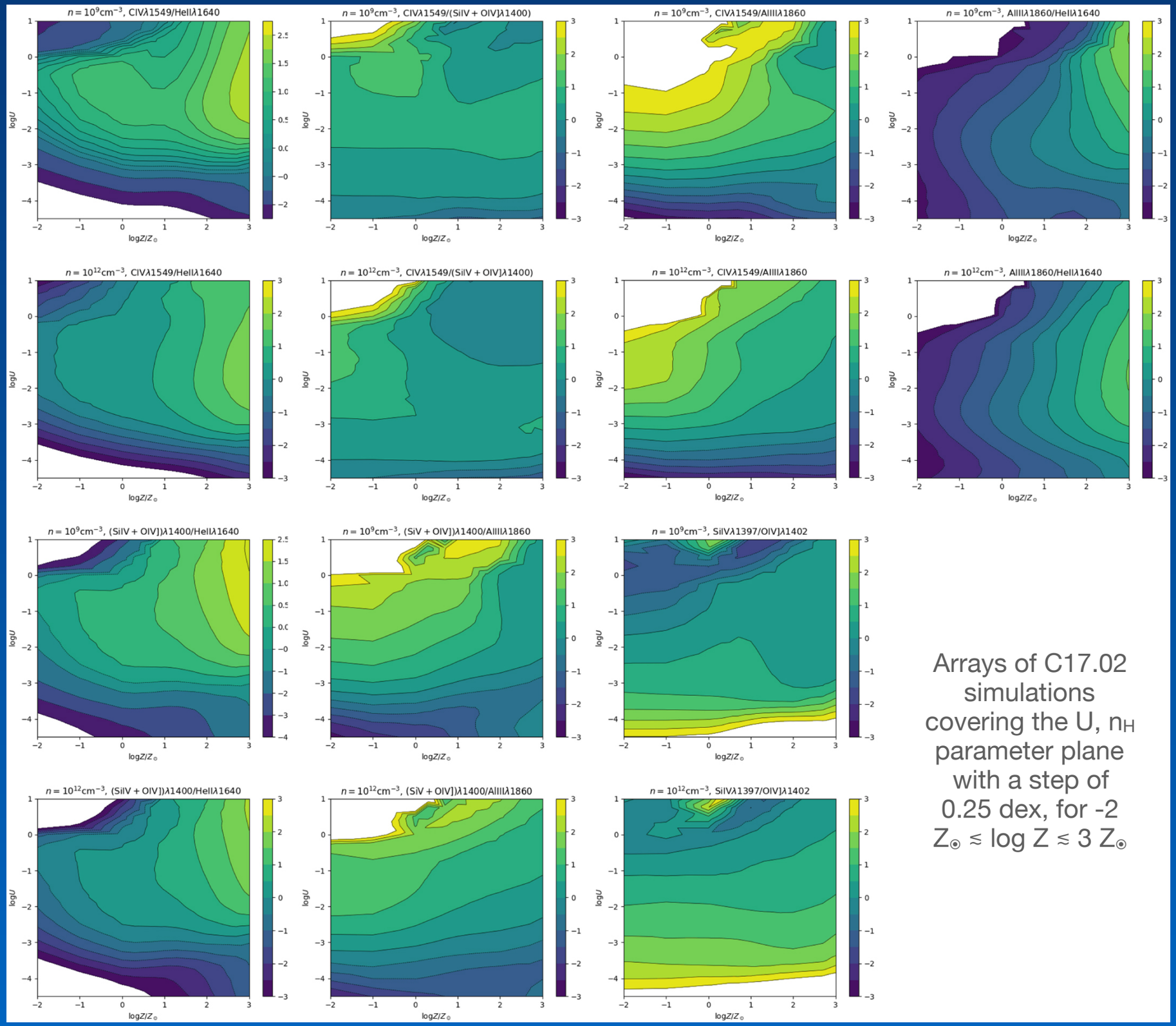

Arrays of C17.02 simulations covering the U, n_H parameter plane with a step of 0.25 dex, for -2 $Z_\odot \lesssim \log Z \lesssim 3\ Z_\odot$

Sniegowska et al. 2021

Extreme Population A: Very homogeneous properties and extreme values of metallicity (Z≳20 $Z_\odot$)

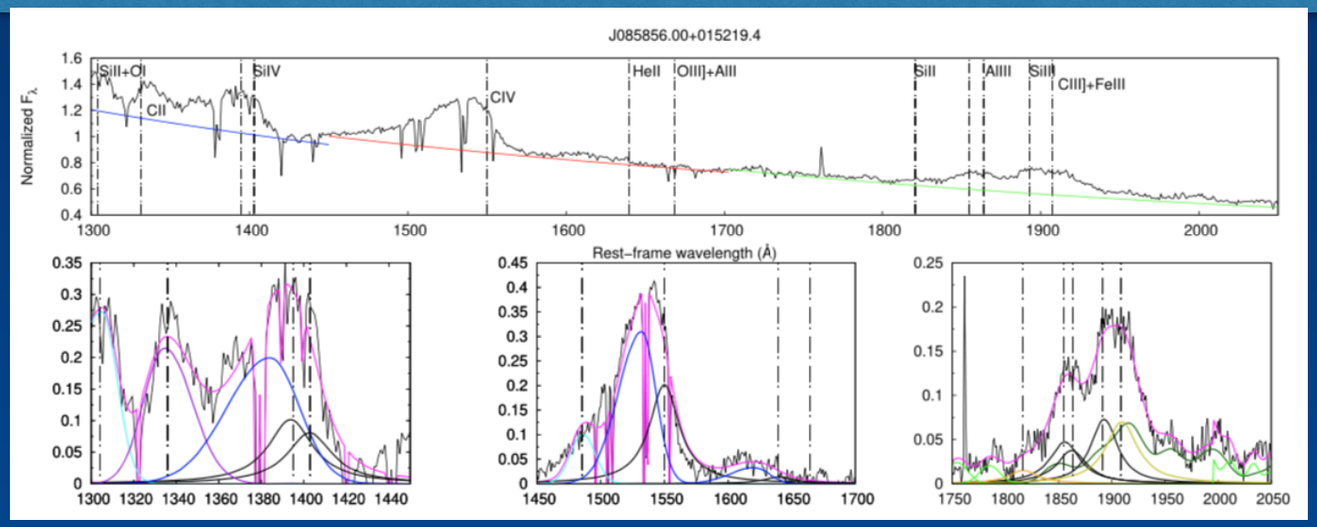

Free n_H, U

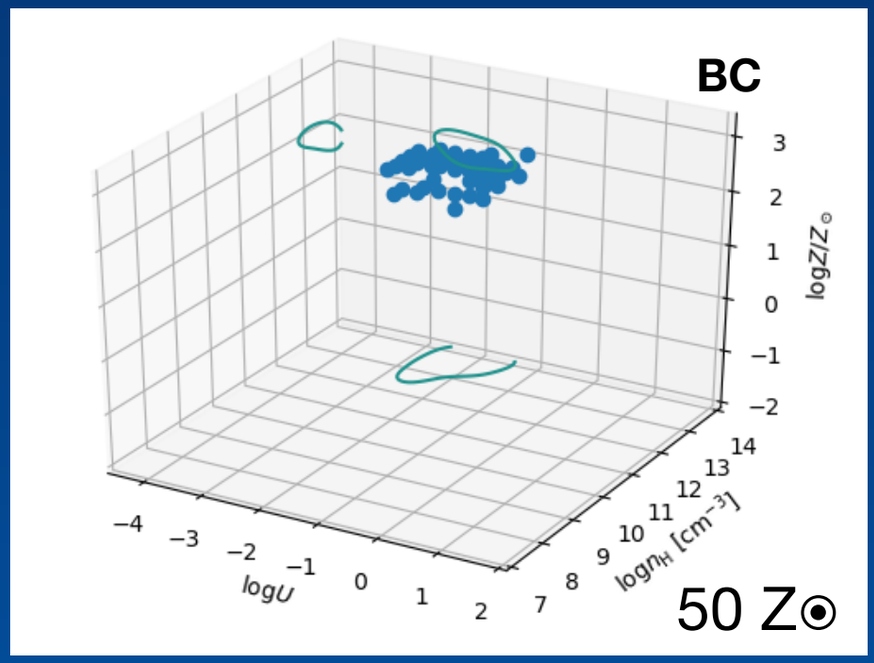

For the low-ionizaton BLR, ionization parameter, density, and Z are constrained

Systematic Z differences from different diagnostics?

Fixed n_H, U: BC

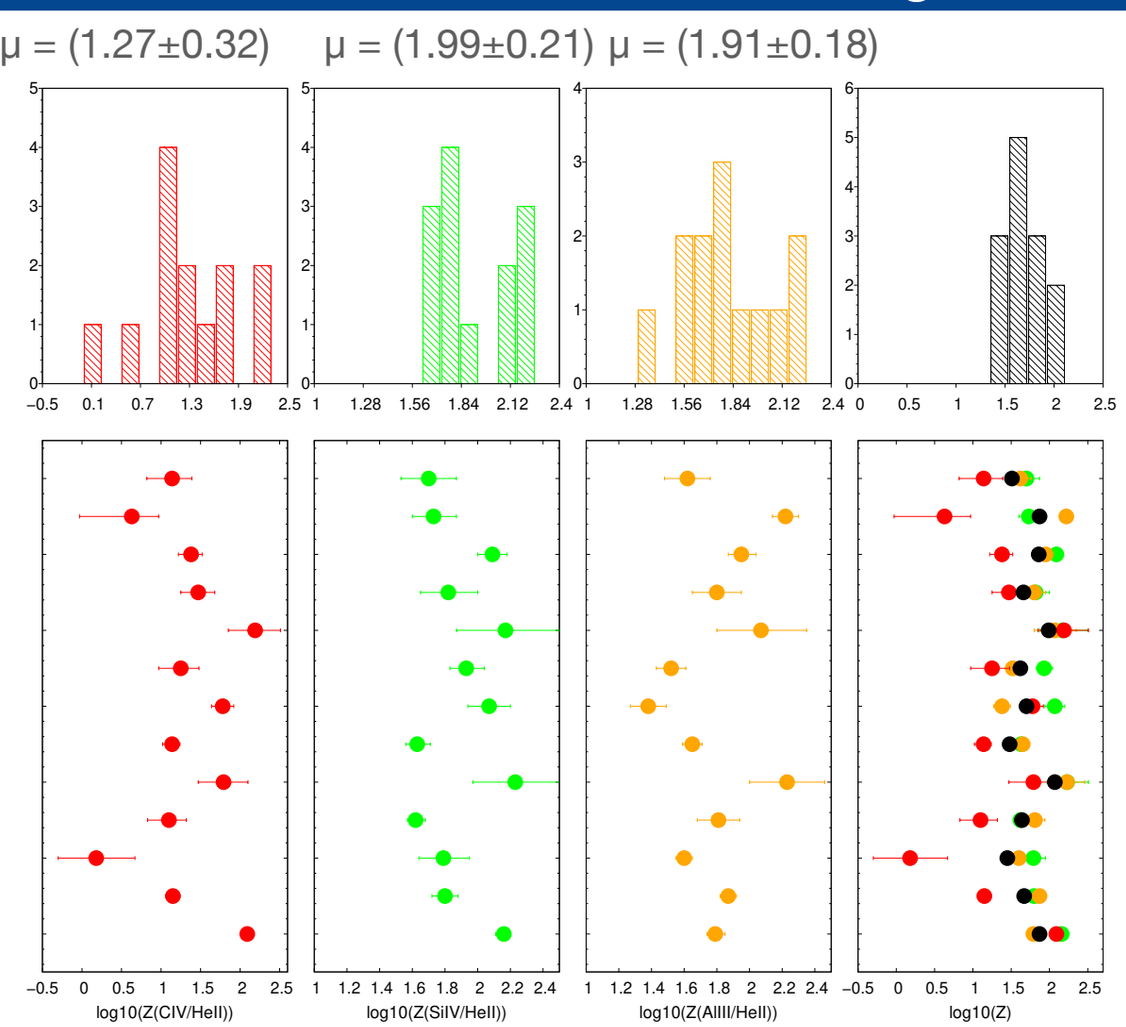

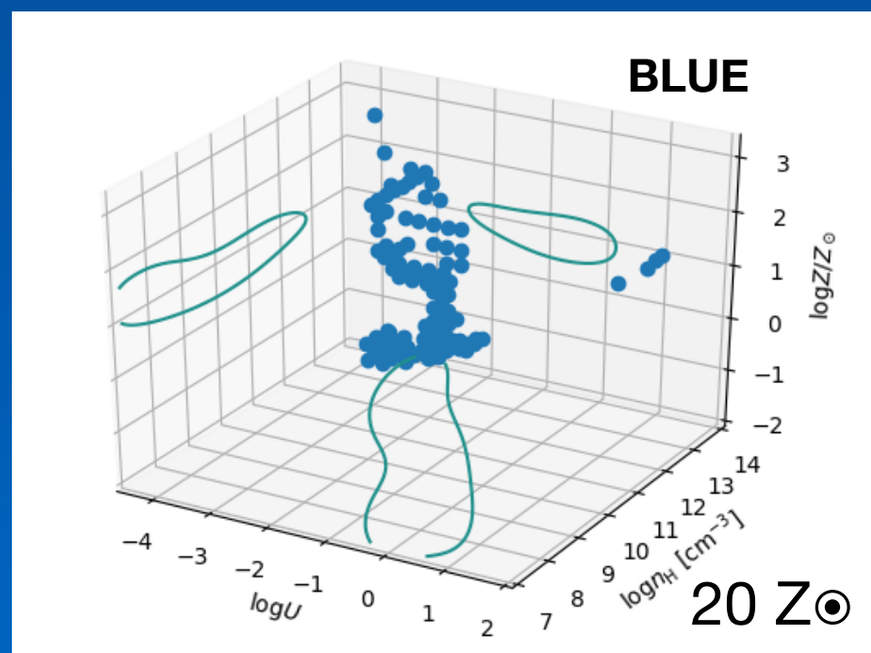

(Negrete et al. 2012; Martínez-Aldama et al. 2018; Sniegowska et al. 2021

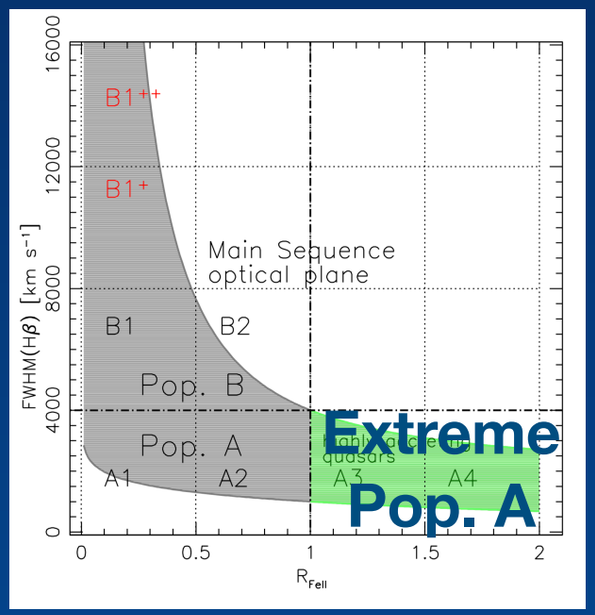

Systematic differences imply over-abundances of Al and Si with respect to C

Z(CIV/HeII) ~ 10 Z⊙

Z(AlIII/HeII) ~ 20 - 50 Z⊙

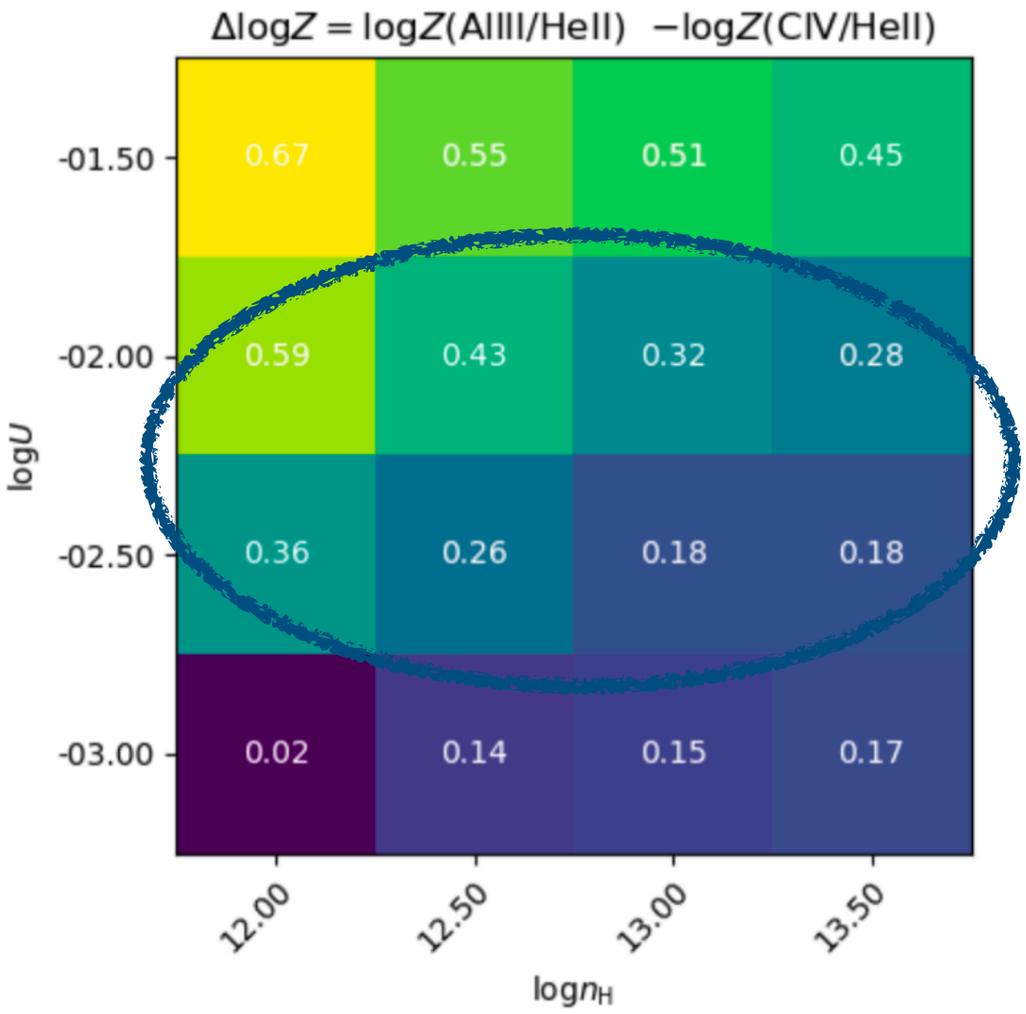

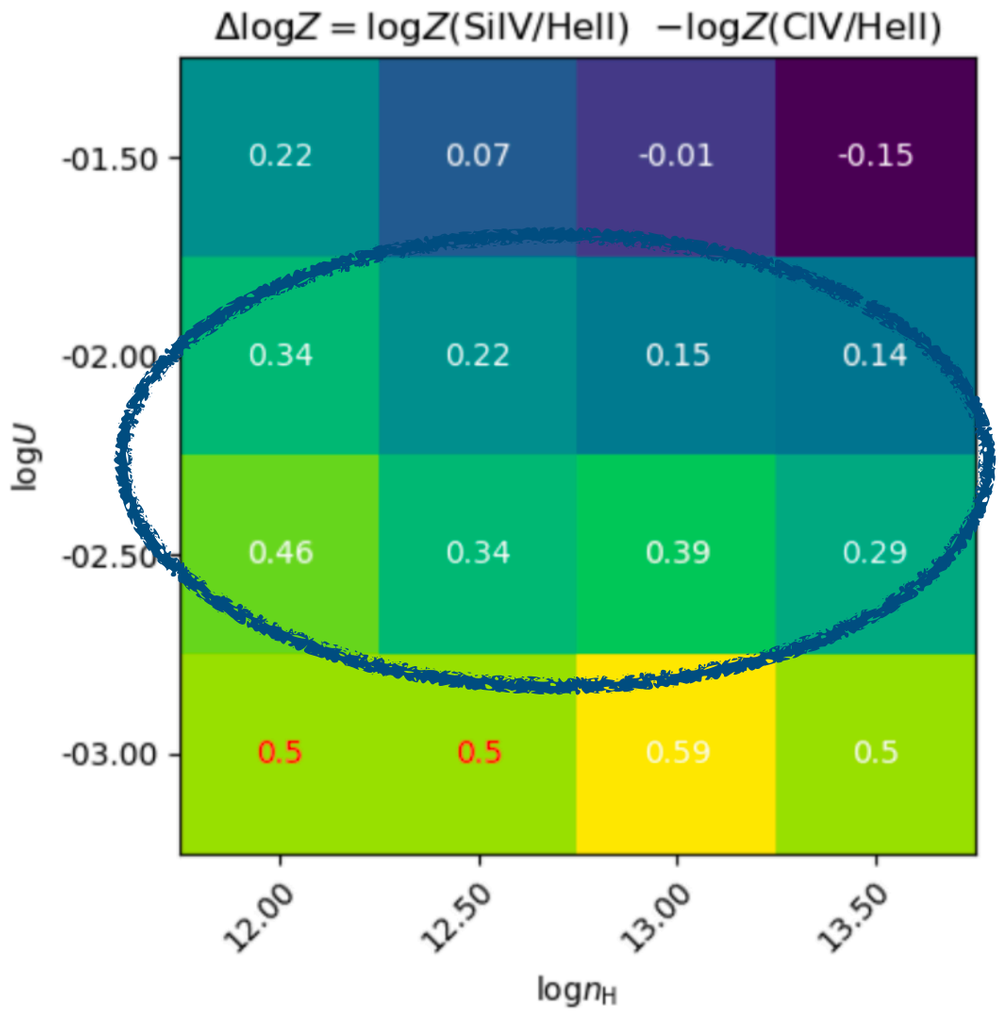

Enlarged sample of 39 objects by Garnica et al., in preparation, and poster on display)

The xA can reach very high radio power $P_\nu \sim 10^{25}$ W Hz^{-1}

xA follows the correlation SFR from FIR - SFR from radio observed for radio-quiet quasars: radio power from supernova remnants

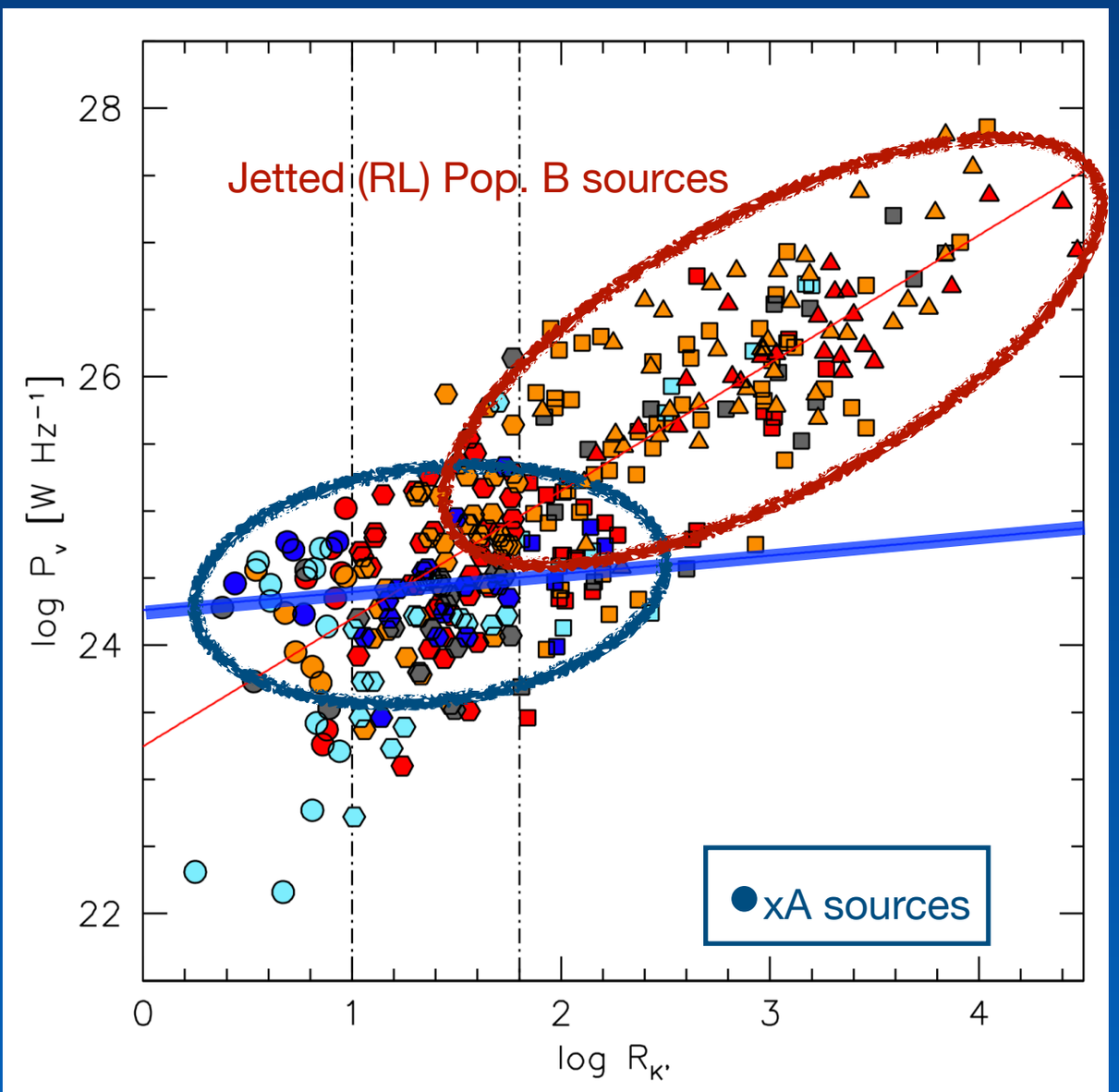

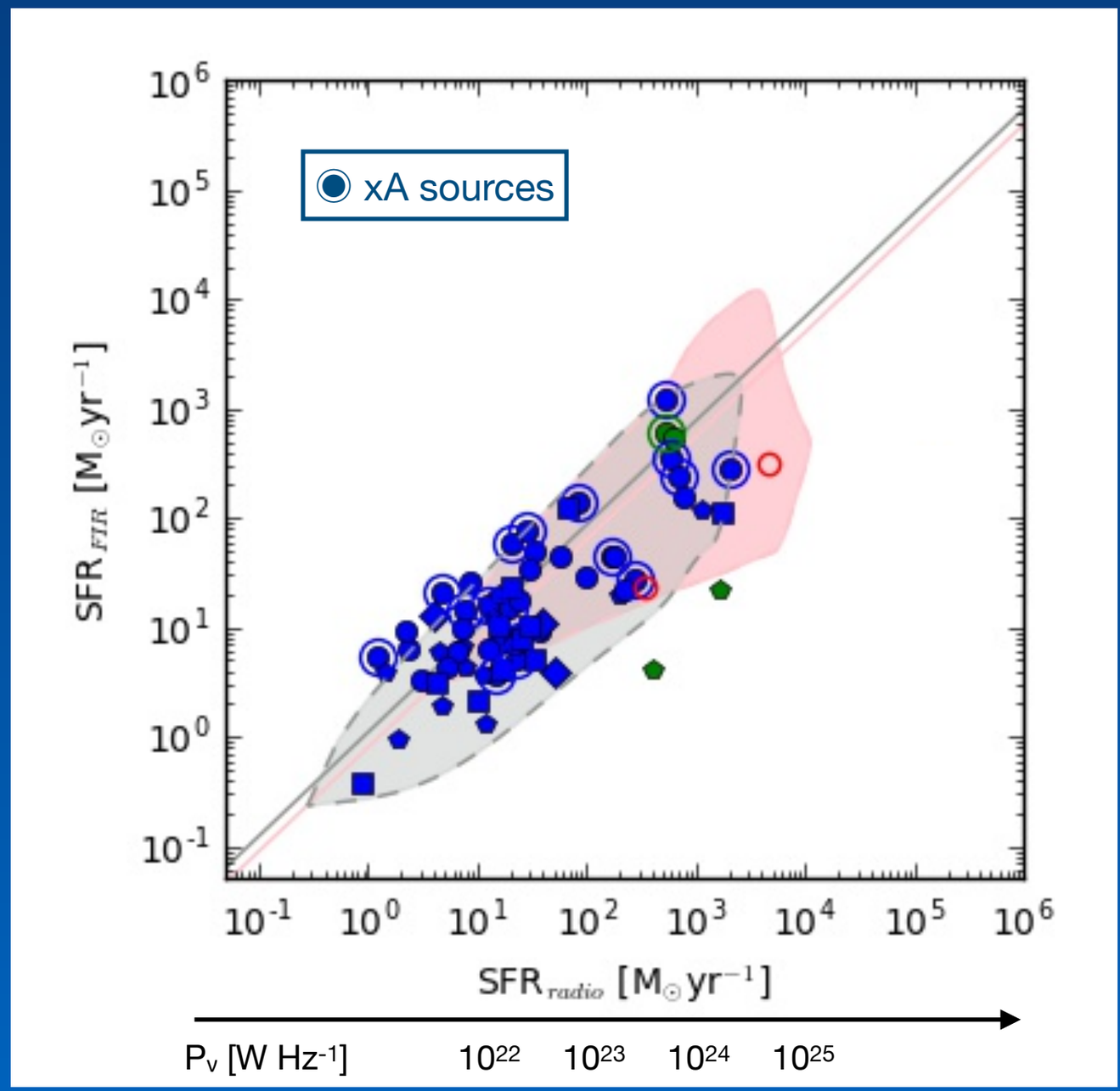

Ganci et al. 2019; del Olmo et al. 2021; cf. Bonzini et al. 2015

xA in a particular stage of quasar evolution
Pollution of the line emitting gas by core-collapse supernovae

Enrichment
via SN II/Ibc

Enriched
Fuel

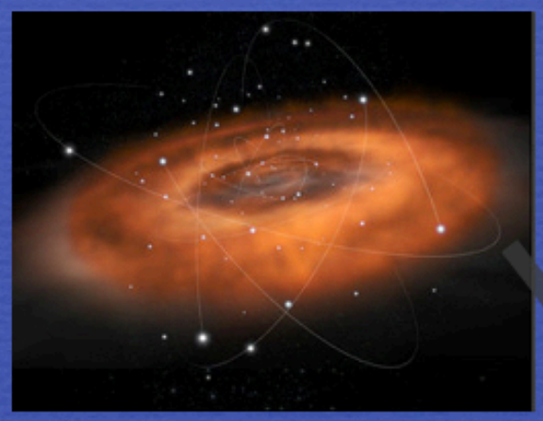

Feedback: Highly accreting quasars, $L/L_{Edd} \sim 1$, with powerful winds, very metal rich

D'Onofrio et al. 2020

Population B, Population A, xA in different accretion modes

Interplay between the Broad Line Region and the structures are associated with different accretion modes still to be clarified

D'Onofrio et al. 2021; Giustini and Proga 2019

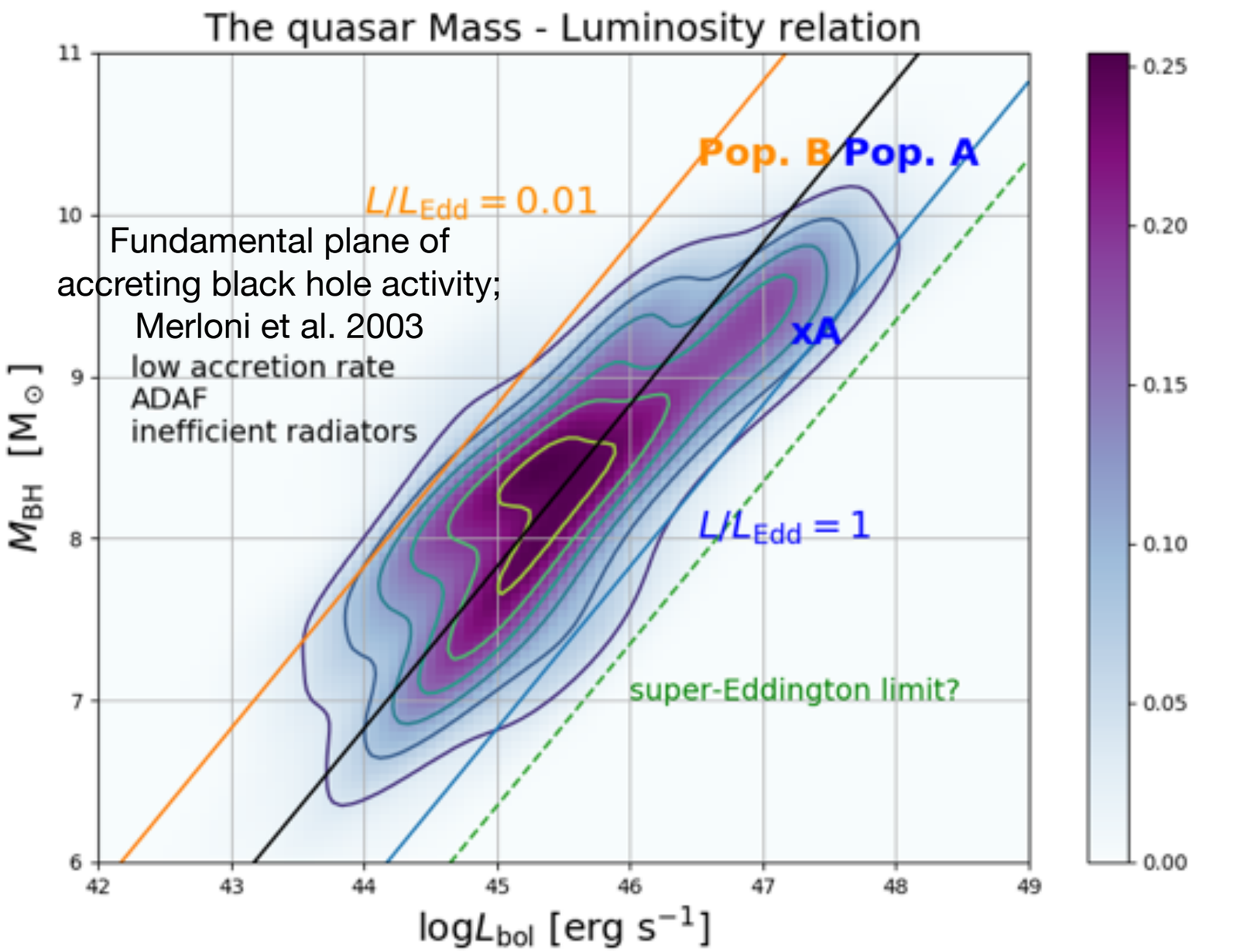

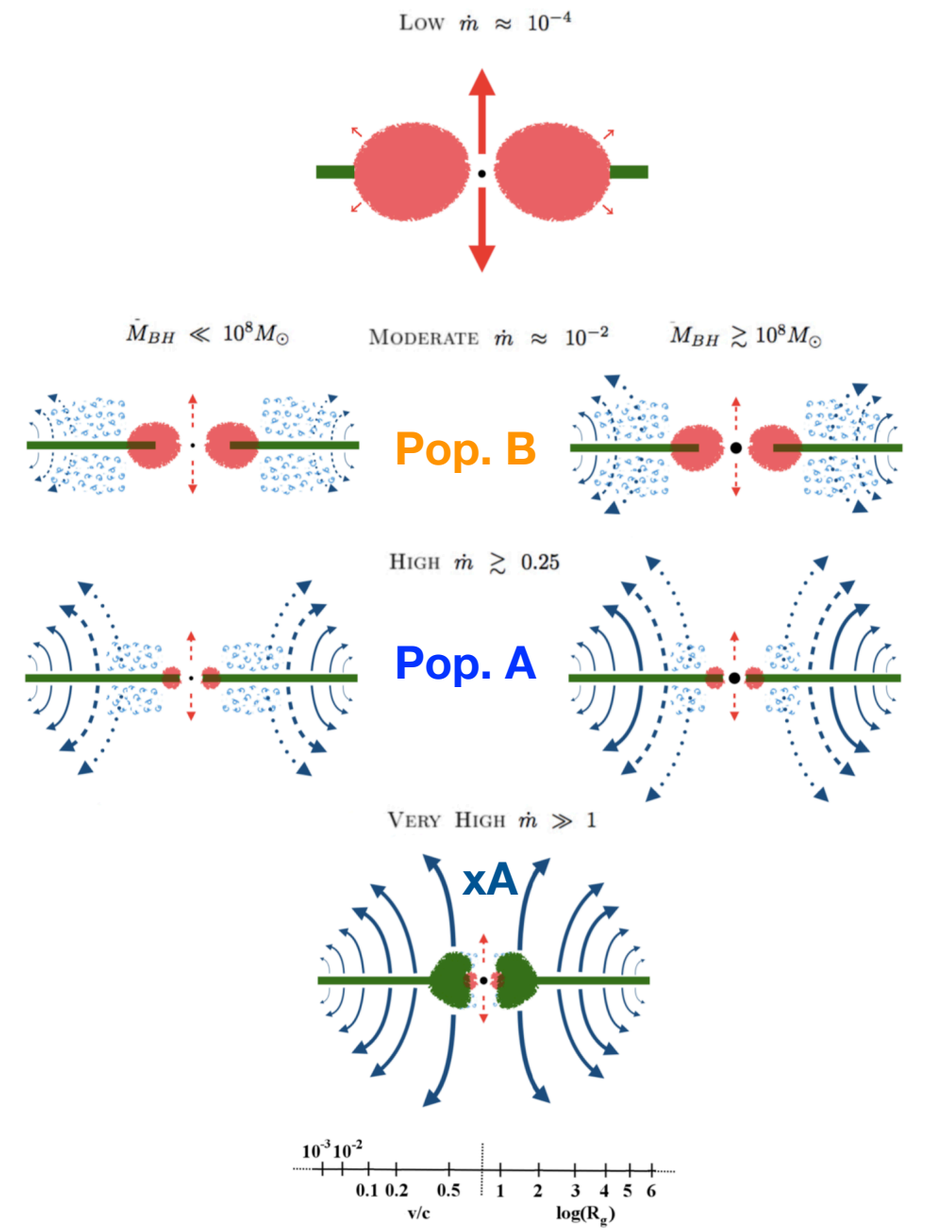

Conclusions

- Recent developments strengthen the interpretation of the MS quasars based on Eddington ratio and orientation

- Population B extreme: "disk dominated;" the flatness of the emitting region helped detect orientation effects

- The MS is not only about spectral parameters; instead, it reflects different evolutionary and environmental situations

- Extreme of Population A: very metal rich, possibly with enrichment associated with a circumnuclear Starburst
  Possible "Eddington standard candles?"
  (talk by Tania Buendia Rios)

- Automatic recognition of large xA samples via machine learning

(e.g. Peruzzi et al. 2021)